CLASSICAL DYNAMICS STUDY OF INTRAMOLECULAR ENERGY TRANSFER IN BENZENE

By

KAREN LYNN BINTZ

Bachelor of Science

Northeastern Oklahoma State University

Tahlequah, Oklahoma

1984

Submitted to the Faculty of the
Graduate College of the
Oklahoma State University
in partial fulfillment of
the requirements for
the Degree of
MASTER OF SCIENCE
December, 1986

CLASSICAL DYNAMICS STUDY OF

INTRAMOLECULAR ENERGY

TRANSFER IN BENZENE

Thesis Approved:

Donald L. Thompson
Thesis Adviser

Wm J Scott

Paul Westhaus

Lionel M. Raff

Norman N. Durham
Dean of the Graduate College

PREFACE

Classical trajectory calculations have been carried out to investigate intramolecular energy transfer in benzene. The effect of anharmonicity on energy transfer from an excited CH stretch local mode has been explored. A general code has been developed in conjunction with this study that can be used to treat other molecular systems with a minimum of programming effort.

I wish to express my sincere gratitude to my research adviser, Dr. Donald L. Thompson, for all of his support and encouragement throughout this study. I am also thankful to my committee, Dr. Lionel Raff, Dr. Paul Westhaus, and Dr. Larry Scott, for their time and advisement.

I wish to express sincere appreciation to Dr. John Brady, Cornell University, for his assistance in this work and for his support during my stay at Cornell University.

This research was supported in part by the U. S. Army Research Office for which I am most thankful. I want to thank John W. Skinner for his support through the Skinner Fellowship program. I also wish to thank the Doctors' Hospital Auxiliary for a scholarship.

Special thanks and gratitude are also due my husband, Daniel Bintz, for his support, encouragement, and understanding throughout the duration of my study at Oklahoma

State University. I also want to express my sincere appreciation to him for the many late hours he spent helping me edit and copy this manuscript.

TABLE OF CONTENTS

LIST OF TABLES

LIST OF FIGURES

Figure Page

CHAPTER I

INTRODUCTION

A. Literature Review

A variety of mechanisms have been advanced to explain the rapid rate of intramolecular vibrational relaxation observed subsequent to overtone excitation of CH bonds in benzene. Resonance interactions, especially the Fermi resonance between an excited CH bond and the associated CCH wag, have generally been advanced as instrumental in enhancing the rate of energy transfer from the excited CH bond. However, other mechanisms have been proposed which involve rapid decay of energy from the excited CH bond via overtone to combination-state decay pathways. Cerjan, Shi and Miller (1) and Shi and Miller (2) have reported theoretical studies of line shapes of CH stretch overtones in benzene in which they discuss the decay of energy from the excited CH bond in terms of resonance interactions. The model employed by Shi and Miller (2) arises from a combination of the semiclassical perturbation approximation and a kinetic coupling model. Their model produces results which are in reasonable agreement with experimental line shapes of CH stretch overtones in benzene. Several other theoretical studies have also reported numerical techniques

for calculation of CH overtone line shapes in benzene (3,4). Heller and Mukamel (3) have concluded that the width of the $|v,0,0,0,0,0\rangle$ overtone state is dependent on the width of the $|v-1,1,0,0,0,0\rangle$ combination state lending support to an overtone-to-combination decay mechanism. In contrast, Buch, Gerber, and Ratner (4) have concluded that their model for calculating CH overtone line shapes in benzene supports a CH stretch to CCH wag decay mechanism.

Sibert *et al.* (5,6,7,8) have reported both classical and quantum mechanical studies which discuss the decay of energy from overtone excitations of CH bonds in the context of resonance interactions. They have used classical nonlinear perturbation theory to demonstrate the relationship between nonlinear resonances and the observed rapid decay of energy from CH stretches. They have concluded that energy decays rapidly from an excited CH stretch local mode into the ring modes "through a succession of many overlapping zones of nonlinear resonance" (5) with a Fermi resonance between the CH stretch and the in-plane CCH wag being instrumental in facilitating the rapid rate of energy transfer out of the CH bond. This result is in qualitative agreement with the results of their companion quantum mechanical study in which they also found that energy decay proceeded through a Fermi resonance between the CH stretch and the in-plane degrees of freedom. Stannard and Gelbart (9) have reported a theoretical study of intramolecular vibrational energy

redistribution in benzene which demonstrates enhanced energy flow from combination states relative to overtone states indicating that a transition from an overtone state to a combination state should expedite the rate of energy flow from an excited CH bond. However, as noted by Stannard and Gelbart (9), that study neglects potential-energy coupling between the CH stretches and the bath modes and thus precludes the possibility of resonance interactions between these modes. Also, they suggest that inclusion of potential-energy coupling could open up energy flow pathways via resonance interactions between the CH stretch and the CCH bend modes thereby preempting the overtone to combination decay. Stannard and Gelbart (9) have also proposed the existence of two sets of bath modes: one set interacts strongly with the CH stretch local modes and the other set interacts only weakly. This suggests the existence of specific state-to-state pathways through which intramolecular vibrational relaxation occurs.

Reddy, Heller, and Berry (10) proposed and tested several possible mechanisms for energy flow from overtone excitations of CH bonds. They concluded on the basis of their analysis of the the spectral line widths and shapes that specific dynamical (i.e., state-to-state) intramolecular rate processes occur in benzene. Their analysis, which is based on information theory, indicates that nonsimultaneous decay models yield results which are in reasonable accord with experimental observations whereas

a simultaneous decay (i.e., statistical) model "never" yields reasonable qualitative results. Their observations lend support to a mechanism in which only a subset of the available degrees of freedom directly participate in the rapid decay of energy from an excited CH bond. Reddy et al. (10) also discussed the importance of coupling between bond mode states relative to coupling between bond mode states and bath states. In agreement with similar observations by Stannard et al. (9), Reddy et al. (10) proposed that the first step in a sequence of state-to-state relaxation processes may be the transfer of one quantum of energy between CH oscillator bond-mode states rather than transfer from a bond-mode state into the bath states. If combination states decay faster than does the corresponding overtone state, this mechanism would enhance the rate of energy flow. However, Reddy et al. (10) have employed direct one-photon absorption techniques in the preparation of the CH overtone states. This method has been the subject of recent criticism (9,11,12,13). Holme and Hutchinson (11) have noted that in polyatomic molecules intramolecular vibrational relaxation occurs much faster than does excitation. As energy is absorbed by a local mode, it is almost simultaneously relaxing into eigenstates which project onto that local mode. This suggests that it is not experimentally feasible to prepare overtones by photochemical activation using a single laser. Holme and Hutchinson (11) have suggested, however, that by building a

superposition of two eigenstates using two lasers, localized excitations might be achieved.

Another point of discussion has been the relative importance of the density of states in energy redistribution. Sibert et al. (5) suggested that the total density of states is not critical in relation to the rate of intramolecular energy transfer. However, as discussed by Parmenter (14), for a given system in an electronically excited state it appears that a critical threshold must be reached before intramolecular vibrational randomization occurs. Studies by Hopkins, Langridge-Smith, and Smalley (15) show that no significant differences exist in the intramolecular vibrational randomization data obtained for the ground and first-excited states of alkylbenzenes. Smalley et al. (15,16) have also concluded that the only barrier to rapid vibrational energy randomization is an inadequate density of states. Swamy and Hase (17) have shown that there is an "extension of localized wave functions for bound vibrational states into the vibrational continuum" for the model reaction H-C-C --> H + C=C thereby indicating that complete energy randomization may not occur even in regions of very high state density. Reddy et al. (10) have noted nearly equivalent $5\nu_{CH}$ bandwidths for toluene and benzene indicating that the density of states may not be crucial to the energy redistribution process at this level of excitation. McDonald (18) summarized state dependencies over the range of state densities noting that

at low state densities completely state-specific effects are expected with less and less selectivity occurring as the state densities increase. The question of the effect of state densities on intramolecular energy transfer does not appear to be settled at this time.

Another factor which must be considered in examining the overall problem of intramolecular vibrational energy redistribution is the effect of rotation-vibration mixing. Studies by Hopkins et al. (15) and by Stewart and McDonald (19) indicate that low thresholds exist in the ground electronic state of benzene. As pointed out by Parmenter (14), rotation-vibration mixing is often operative in systems with low thresholds. It would therefore be reasonable to expect that inclusion of rotational effects might further enhance the rate of energy flow from an excited CH stretch.

B. Scope of Study

The scope of this study is to examine intramolecular energy transfer in benzene employing classical trajectory calculations. Of specific interest is the rate and mechanism of energy transfer from an initially excited CH bond. Both harmonic and anharmonic potential-energy surfaces are employed to determine the effect of anharmonicity on energy flow from an excited CH bond. The importance of employing anharmonic forms for XH bond potentials (where the X atom mass is significantly greater

than the H atom mass, such as for CH bonds) has been discussed in other studies concerned with the rates and mechanisms of intramolecular energy transfer (5,20,21,22). However, results are obtained in this study which indicate that the rate of energy transfer from an excited CH bond in benzene is also dependent upon the form of the potential-energy surface and not just upon the anharmonicity of the CH bond of interest.

The mechanism by which energy transfer occurs is also addressed. The results predict the existence of two distinct sets of bath modes as discussed by Stannard and Gelbart (9). As expected, the results also indicate a correlation between the rate of energy transfer out of the excited CH bond and the relative frequencies of the CH bond and the associated in-plane CCH wag angles. Other aspects of the mechanism which should be addressed, but are beyond the scope of this study, are the overtone-combination decay mechanism and the importance of Coriolis coupling.

The primary focus of this study is intramolecular energy transfer in benzene. However, the topic of intramolecular energy transfer, as it relates to molecular systems in general, is interesting in its own right. In an attempt to address questions relating to this topic with a minimum of time spent on programming and program implementation, a general classical trajectory code has been developed in conjunction with this study of benzene. The code can be used to treat energy transfer in other

molecules with a minimum of modification and programming time. This code is discussed in detail in Chapter 2.

Chapter 2 discusses the methods which are employed in the calculations including use of the general classical trajectory code, Chapter 3 describes the potential-energy surfaces, Chapter 4 deals with the results and discussion, and Chapter 5 gives the conclusions of the study.

CHAPTER II

METHODS

A. Introduction

A new general classical trajectory code was developed and used for this study of intramolecular benzene dynamics. The code is intended to be general enough to permit calculation of trajectories and energy transfer results for most molecules without requiring major revision. The prohibiting factor in the use of this code is the amount of CPU time required for integration of the equations of motion. Calculations for the benzene study required as much as four days of DEC VAX 11/780 CPU time for an ensemble of 50 trajectories which were each allowed to run for two picoseconds with a stepsize of 4.89×10^{-17} s. The code contains seven basic sections:

i. Input
ii. Determination of equilibrium geometry
iii. Normal mode analysis
iv. Initial conditions selection
v. Calculation of the potential energy and derivatives
vi. Integration of the equations of motion
vii. Final state analysis.

Each of the sections is described in more detail in Sections II.B. through II.H.

The following modifications in the code are required to accommodate a particular molecule:

i. Development of an input data file which is compatible with the input section of the code. A more detailed description of the input requirements is given in Section II.B.

ii. A subroutine must be written, in a format compatible with the code, to provide the equilibrium geometry of the molecule.

iii. The final state analysis is currently limited to calculation of the energy in X-H type bonds and/or calculation of the energy in the normal modes of the molecule as a function of time. Modifications can be made to expand the scope of the final state analysis.

It is also possible to upgrade the code to incorporate other specific capabilities. The present format of the program consists of a driver program which uses call statements to access individual program modules (subroutines) to carry out specific tasks (e.g. normal mode analysis). New options can be included employing new call statements and subroutines without affecting the operation of the existing program. However, consistancy must be maintained in common blocks and variable name assignments.

B. Input

The INPUT subroutine reads the molecule's structural information from a data file which is specific to the molecule under consideration. The subroutine requires information about the number of atoms, bonds, bond angles, dihedral angles, and "wag" angles in the molecule. This information is then used by the subroutine to determine how to read the next section of the data file. The next section of the data file consists of information pertaining to specific atoms, bonds, and angles such as atomic weights, equilibrium bond lengths and angles, and which atoms participate in each bond and angle. The next section of the data file contains information pertaining to the potential-energy surface of the molecule. Each potential interaction is assigned a type number as shown in Table I. Therefore the data file must contain the number of desired interactions of each potential type. The remainder of the data file conveys information about which bonds and angles are involved in each of the potential interactions and the potential parameters for each interaction. An example data set for benzene is shown in Table II. This example potential for benzene consists of Morse functions for the 12 bonds, harmonic angle potentials for the 18 bond angles, and no potential interactions for the wags or dihedrals.

TABLE I

POTENTIAL INTERACTIONS BY "TYPE NUMBER"

Type Number	Potential Interaction
1	$kR^2/2$
2	kR_1R_2 (R_1 and R_2 adjacent bonds)
3	kR_1R_3 (R_1 and R_3 nonadjacent bonds)
4	Morse bond potential
5-7	unassigned
20	$k\theta^2/2$ (θ = bond angle)
21	$k\gamma^2/2$ (γ = wag angle)
22	$\sum_i a_i \cos(i\phi_j)$ (ϕ_j= dihedral angle)
23-26	unassigned

TABLE II

EXAMPLE DATA SET OF BENZENE POTENTIAL PARAMETERS

12	12	18	6	6	No. of atoms, bonds, and angles
				12.0000	Atomic weight of each atom.
				1.0008	
				12.0000	
				1.0008	
				12.0000	
				1.0008	
				12.0000	
				1.0008	
				12.0000	
				1.0008	
				12.0000	
				1.0008	
1	2			1.0840	Atoms involved in each bond
1	3			1.3970	and equilibrium internuclear
3	4			1.0840	distance
3	5			1.3970	
5	6			1.0840	
5	7			1.3970	
7	8			1.0840	
7	9			1.3970	
9	10			1.0840	
9	11			1.3970	
11	12			1.0840	

TABLE II (Continued)

```
11  1          1.3970
11  1  3     120.0000  Atoms involved in each  bond angle
11  1  2     120.0000  and equilibrium angle in degrees
 2  1  3     120.0000
 1  3  5     120.0000
 1  3  4     120.0000
 4  3  5     120.0000
 3  5  7     120.0000
 3  5  6     120.0000
 6  5  7     120.0000
 5  7  9     120.0000
 5  7  8     120.0000
 8  7  9     120.0000
 7  9 11     120.0000
 7  9 10     120.0000
10  9 11     120.0000
 9 11  1     120.0000
 9 11 12     120.0000
12 11  1     120.0000
11  1  3  2  1       0.0000 Atoms and bond angle
 1  3  5  4  4       0.0000 involved in each wag angle
 3  5  7  6  7       0.0000 and equilibrium wag angle
 5  7  9  8 10       0.0000 in degrees
 7  9 11 10 13       0.0000
 9 11  1 12 16       0.0000
11  1  3  5  1  4       0.0000  Atoms and the two bond
```

TABLE II (Continued)

1	3	5	7	4	7		0.0000	angles involved in each
3	5	7	9	7	10		0.0000	dihedral angle and the
5	7	9	11	10	13		0.0000	equilibrium dihedral
7	9	11	1	13	16		0.0000	angle in degrees
9	11	1	3	16	1		0.0000	
0	0	0	12	0	0	0	No. of interactions--types 1-7	
18	6	6	0	0	0	0	No. of interactions--types 20-26	
4	1			1.8700			105.0000	Interaction type no.,
4	2			2.0540			130.0000	bond no., Morse
4	3			1.8700			105.0000	parameters--Beta and
4	4			2.0540			130.0000	D_e.
4	5			1.8700			105.0000	
4	6			2.0540			130.0000	
4	7			1.8700			105.0000	
4	8			2.0540			130.0000	
4	9			1.8700			105.0000	
4	10			2.0540			130.0000	
4	11			1.8700			105.0000	
4	12			2.0540			130.0000	
20	1	1		181.0000				Interaction type no.,
20	2	2		34.6500				angle nos., potential
20	3	3		34.6500				parameter
20	4	4		181.0000				
20	5	5		34.6500				
20	6	6		34.6500				
20	7	7		181.0000				

TABLE II (Continued)

20	8	8	34.6500
20	9	9	34.6500
20	10	10	181.0000
20	11	11	34.6500
20	12	12	34.6500
20	13	13	181.0000
20	14	14	34.6500
20	15	15	34.6500
20	16	16	181.0000
20	17	17	34.6500
20	18	18	34.6500

A second input subroutine, VARY, is used to read information from a data file concerning the details of a specific trajectory calculation. Table III gives an example data file for benzene along with an explanation of each line in the file.

TABLE III

EXAMPLE DATA SET OF PARAMETERS FOR A SPECIFIC TRAJECTORY CALCULATION

.0010 40.0000 1	DT, CUTOFF, TRAJNO*
50.0000 00	Energy above the ground state energy
00.0000 00	to be assigned to an excited bond,
00.0000 00	quantum number for an excited bond.
00.0000 00	NOTE: Only one of the fields may be
00.0000 00	used per bond.
00.0000 00	
00.0000 00	
00.0000 00	
00.0000 00	
00.0000 00	
00.0000 00	
00.0000 00	
0 0 0 0 0 0 0 0 0 0 0 0 0 0 0 0 0 0 0 0	Quantum numbers
0 0 0 0 0 0 0 0 0 0 0 0 0 0 0 0 0 0 0 0	for excitation of
0 0 0 0 0 0 0 0 0 0 0 0 0 0 0 0 0 0 0 0	of normal modes.
0 0 0 0 0 0 0 0 0 0 0 0 0 0 0 0 0 0 0 0	
21	Seed number for random number generation
5	Energy is calculated every nth integration step
7	First normal mode to be used in calculations

*DT is the integration step size, CUTOFF is the time cutoff for integration, and TRAJNO is the ensemble size.

C. Determination of Equilibrium Geometry

The equilibrium geometry is determined for each molecule employing basic classical mechanics techniques for coordinate system transformations. Experimental data for equilibrium bond lengths and bond angles is obtained from the literature. The origin of the coordinate system is set at a convenient point (usually at one of the atoms). Coordinates for the remaining atoms are determined by placing an atom on an axis of the coordinate system at a distance equal to the appropriate bond length from an adjacent atom for which the cartesian coordinates have already been determined (such as the atom that is at the origin). The atom is then given its proper orientation relative to the coordinate system by rotating it through the Euler angles using the Euler rotation matrices. (See Goldstein (23) for a discussion of the theory and use of Euler rotation matrices.) This procedure is repeated for each atom in the system, thereby defining the equilibrium geometry. A final translation is then carried out such that the origin of the coordinate system is at the center of mass of the molecule as required for the normal mode analysis (24). The coordinates of the center of mass of the molecule are determined as follows:

$$\begin{aligned} X &= \sum_i m_i x_i / \sum_i m_i \\ Y &= \sum_i m_i y_i / \sum_i m_i \\ Z &= \sum_i m_i z_i / \sum_i m_i \end{aligned} \qquad (1)$$

where X, Y, and Z represent the cartesian coordinates of the center of mass, m_i is the mass of atom i, and x_i, y_i, and z_i are the cartesian coordinates of atom i.

D. Normal Mode Analysis

The formalism described in Wilson, Decius, and Cross (24) is used for the normal mode analysis. The derivation from which the secular equation is obtained is given in Chapter 2 of Wilson, Decius, and Cross (24). The force constant matrix is formed from the mass weighted analytical second derivatives of the potential function. The analytical derivatives are straightforward for most potential interaction terms. However, singularities arise in the evaluation of the first and second analytical derivatives of potential interactions involving dihedral angles. The singularities occur in the evaluation of the derivatives at 0 and 2π radians due to the occurance of a $\sin\phi$ term in the denominator of the derivatives. The singularity can be eliminated when potential interactions of the form

$$V\phi_j = \sum_i a_i \cos(i\,\phi_j) \qquad (2)$$

are used for the dihedral angles, where the ϕ_j are the dihedral angles and the a_i are coefficients which are adjusted to fit the potential to experimental data. The first and second derivatives are determined respectively from

$$\frac{\partial V}{\partial x} = \frac{\partial V_\phi}{\partial \cos\phi} \frac{\partial \cos\phi}{\partial x} \qquad (3)$$

and $\frac{\partial^2 V_\phi}{\partial x \partial y} = \frac{\partial V_\phi}{\partial \cos\phi} \frac{\partial^2 \cos\phi}{\partial x \partial y} + \frac{\partial \cos\phi}{\partial x} \frac{\partial \cos\phi}{\partial y} \frac{\partial^2 V_\phi}{\partial (\cos\phi)^2}$

thereby eliminating the troublesome singularities. The eigenvalues and eigenvectors are obtained by diagonalizing the force constant matrix using the GIVENS diagonalization subroutine. The normal mode frequencies are obtained from the eigenvalues as follows:

$$\nu_i = \sqrt{\lambda_i}/2, \tag{4}$$

where ν_i are the fundamental frequencies of vibration and λ_i are the eigenvalues. The normal coordinate displacement vectors are obtained using a table of transformation coefficients:

	Q_1	Q_2	Q_3	. . . . .	Q_{3N}
q_1	l_{11}	l_{12}	l_{13}	. . . . .	$l_{1,3N}$
q_2	l_{21}	l_{22}	l_{23}	. . . . .	$l_{2,3N}$
q_3	l_{31}	l_{32}	l_{33}	. . . . .	$l_{3,3N}$
.	. . . . .				
.	. . . . .				
q_{3N}	$l_{3N,1}$	. . . . .			$l_{3N,3N}$

, (5)

where the q_i are the mass weighted cartesian displacement coordinates ($q_i = \sqrt{m_j}\Delta x_j$, $q_{i+1} = \sqrt{m_j}\Delta y_j$, $q_{i+2} = \sqrt{m_j}\Delta z_j$) (i=1,3N; N=number of atoms in the molecule), Q_k (k=1,3N) are the normal coordinates, and the columns of the coefficient table are the eigenvectors of the diagnolized force constant matrix corresponding to the respective normal coordinates (24). The normal coordinate displacement

vectors for each normal mode are obtained from the table by multiplying each of the normal coordinates times the respective coefficients:

$$q_i = l_{ik} Q_k \tag{6}$$

where the q_i (i=1,3N) are the mass weighted cartesian coordinates from which the vectors corresponding to normal mode number k (k=1,3N) can be determined. The table can be employed to determine the mass-weighted cartesian displacement coordinates corresponding to a particular phase of the normal coordinates as follows:

$$q_i = \sum_k l_{ik} Q_k \tag{7}$$

with q_i, l_{ik}, and Q_k defined as for Equation (5). The transformation from mass-weighted cartesian displacement coordinates to normal coordinates is accomplished using the inverse transformation:

$$Q_k = \sum_i l_{ik} q_i \tag{8}$$

with q_i, l_{ik}, and Q_k defined as for Equation (5).

Each of the normal modes is assigned by drawing pictorial representations of the mode from the mass-weighted cartesian displacement coordinates obtained using Equation (6). The symmetry type of each mode is established using the guidelines in Appendix X of Wilson, Decius, and Cross (24). The assignments for the normal modes are used to fit the calculated vibrational frequencies for a particular potential to experimental data by methodically changing the force constants and comparing the calculated and experimental frequencies until the best

fit is achieved.

E. Initial Conditions Selection

Initial conditions selection is accomplished by populating each of the normal modes of the molecule with its ground-state vibrational energy as calculated from the chosen potentials and then exciting a local CH stretch mode with an arbitrary energy. The normal modes involving dihedral motions were neglected in the selection of the initial conditions. An harmonic approximation to the ground state vibrational energy in each of the normal modes is calculated as follows:

$$E_k = h\nu_k/2, \tag{9}$$

where h is Planck's constant and ν_k is the fundamental vibrational frequency of mode k. Monte Carlo phase averaging is used to obtain a random initial phase for each of the normal coordinates

$$R = R_e - (R_e - \rho_-)\sin(\pi/2 + \pi\xi), \tag{10}$$

where R_e is the equilibrium separation, ρ_- is the classical inner turning point, and ξ is a random number between zero and one. The cartesian coordinates associated with each of the phase-averaged normal coordinates are determined from a coordinate transformation employing Equation (6). The kinetic energy in each mode is the difference between the ground-state energy of the mode and the potential energy as calculated from the classical Hamiltonian employing cartesian coordinates obtained as described above. The

$\dot{Q}_k$'s are obtained from the kinetic energy by the equation:

$$\dot{Q}_k = \pm \sqrt{2T_k}, \tag{11}$$

where T_k is the kinetic energy in mode k. For the highly anharmonic stretching modes, the potential energy as calculated from the Hamiltonian occasionally exceeds the ground-state energy from the harmonic approximation. For the rare cases when this occurs, the conditions are rejected. The cartesian coordinates and conjugate momenta corresponding to the initial state defined by the phase-averaged normal coordinates and conjugate momenta are obtained from a coordinate transformation using Equation (7). The CH bond (all references to CH bonds may be applied to XH type bonds for a more general discussion) is excited by either assigning to the bond an arbitrary amount of energy above the ground-state energy or by assigning n (n is an integer) quanta of energy to the bond. The bond energies are calculated using a local-mode approximation:

$$E_{CH} = P_H^2/2\mu_{CH} + V_{CH}, \tag{12}$$

where P_H is the momentum of the H atom and V_{CH} is the potential function for the CH bond. For potential-energy surfaces which include coupling terms in the CH bond potential, an harmonic approximation is used to calculate the potential energy in the bond:

$$V_{CH} = k_{CH}R_{CH}^2/2 \tag{13}$$

where R_{CH} is the CH bond internuclear distance and k_{CH} is the CH bond harmonic force constant. The CH vibrational phase for a Morse oscillator potential function is selected

as described by Suzakawa, Thompson, Cheng, and Wolfsberg (25),

$$R = R_e + \beta^{-1} \ln \left[\frac{1 - (E_v/D_e)^{1/2} \cos(2\pi\xi)}{1 - (E_v/D_e)} \right] , \quad (14)$$

where D_e and β are the Morse potential well-depth and exponential parameter, respectively, and E_v is the total energy in the oscillator. The CH vibrational phase for a harmonic potential function is selected using Equation (10). The potential energy is calculated and the "excess" energy assigned to kinetic energy. The displacement coordinates and conjugate momenta for the excited bond are added to the coordinates and conjugate momenta determined from the phase-averaged normal coordinates. The process of summing the displacements and momenta along the normal mode and local mode coordinates introduces a molecular angular momentum that must be subtracted out. Using the methods of Hase, Buckowski, and Swamy (26), the rotational velocity ($\vec{\omega} \times \vec{r}_i$) is subtracted from each of the atoms. The assumptions which must be made in the use of ($\vec{\omega} \times \vec{r}_i$) to calculate the linear velocity due to rotation of each of the atoms and a description of practical application of the equation follow.

A radian is defined as "an angle which, if its vertex is placed at the center of a circle, intercepts an arc equal in length to the radius of the circle" (27). From this definition it is immediately obvious that the arc s swept out by an angle θ along the circumference of a

circle of radius R is given by $s=R\theta$ when θ is measured in radians. Differentiating this equation for s with respect to time yields:

$$\frac{ds}{dt} = \frac{dR}{dt}\theta + \frac{d\theta}{dt} R \tag{15}$$

Assuming that the radius of the circle (or more generally the radius of rotation of a point mass) is essentially constant, Equation (15) reduces to

$$\frac{ds}{dt} = R \frac{d\theta}{dt}$$

or

$$v = R\omega \tag{16}$$

where v is the linear velocity due to rotation of a point mass traveling along the circumference of a circle of radius R with angular velocity ω . It is also possible to show that

$$\vec{v} = \vec{\omega} \times \vec{r} \tag{17}$$

by beginning with an examination of Figure 1 which represents a point mass rotating with angular velocity $\vec{\omega}$ about a circle of radius $R=r\sin\tau$ with $\vec{r}$ and τ as defined by Figure 1. The orientation of $\vec{v}$ satisfies Equation (17) in that $\vec{v}$ is perpendicular to the plane of $\vec{r}$ and $\vec{\omega}$ and is in the proper direction relative to the right hand rule. But it is also necessary to establish that $|\vec{\omega} \times \vec{r}|$ satisfies $v=R\omega$ as required by Equation (16). From the definition of cross products, $|\vec{\omega} \times \vec{r}| = \omega r\sin\tau$ and from Figure 1 it has already been established that $R=r\sin\tau$, therefore $|\vec{\omega} \times \vec{r}| = R\omega$ as required (28).

In practice Equation (17) is applied by first calculating the angular velocity of the system $\vec{\omega}_s$ which can be determined from the angular momentum of the system $\vec{L}_s$. By definition, the angular momentum of a system of particles about their center of mass is

$$\vec{L}_s = \sum_i (\vec{r}_i \times m_i \vec{v}_i) \tag{18}$$

where $\vec{r}_i$ is the vector that defines the position of particle i relative to the center of mass, m_i is the mass of particle i, and $\vec{v}_i$ is as previously defined (29). Substituting Equation (17) for $\vec{v}_i$ into Equation (18) yields

$$\vec{L}_s = \sum_i m_i \vec{r}_i \times (\vec{\omega}_i \times \vec{r}_i) \tag{19}$$

from which the components of the angular momentum L_x, L_y, and L_z can be obtained by carrying out the vector triple products. The result is

$$\begin{aligned} L_x &= \omega_{sx} \sum_i (y_i^2+z_i^2) m_i - \omega_{sy} \sum_i x_i y_i m_i - \omega_{sz} \sum_i x_i z_i m_i \\ L_y &= -\omega_{sx} \sum_i x_i y_i m_i + \omega_{sy} \sum_i (z_i^2+x_i^2) m_i - \omega_{sz} \sum_i y_i z_i m_i \\ L_z &= -\omega_{sx} \sum_i z_i x_i m_i - \omega_{sy} \sum_i y_i z_i m_i + \omega_{sz} \sum_i (x_i^2+y_i^2) m_i \end{aligned} \tag{20}$$

or in matrix notation

$$\begin{pmatrix} L_x \\ L_y \\ L_z \end{pmatrix} = \begin{pmatrix} \sum_i m_i (y_i^2+z_i^2) & -\sum_i x_i y_i m_i & -\sum_i x_i z_i m_i \\ -\sum_i x_i y_i m_i & \sum_i m_i (z_i^2+x_i^2) & -\sum_i y_i z_i m_i \\ -\sum_i z_i x_i m_i & -\sum_i y_i z_i m_i & \sum_i m_i (x_i^2+y_i^2) \end{pmatrix} \begin{pmatrix} \omega_{sx} \\ \omega_{sy} \\ \omega_{sz} \end{pmatrix} \tag{21}$$

or

$$\vec{L}_s = \vec{I}_s \, \vec{\omega}_s \tag{22}$$

where $\vec{I}_s$ is the inertia tensor of the system. Multiplying both sides of Equation (22) by $\vec{I}_s^{-1}$ yields for $\vec{\omega}_s$:

$$\vec{\omega}_s = \vec{I}_s^{-1} \vec{L}_s. \tag{23}$$

The angular velocity of the system $\vec{\omega}_s$ can be calculated

from Equation (23) and then substituted into Equation (17) to determine the linear velocity of each particle in the system due to rotation. This velocity is then subtracted from the initial velocity of each particle to ensure that the system has zero angular momentum.

After the angular momentum has been removed from the system, the coordinates and momenta are scaled to ensure a microcanonical ensemble according to

$$x' = (E^{\circ}_v / Ev)^{1/2}(x - x^{\circ}) + x^{\circ} \quad (24)$$

$$\dot{x}' = (E^{\circ}_v / Ev)^{1/2}\dot{x} \quad (25)$$

where E°_v is the predicted normal-mode energy, E_v is the normal-mode energy as calculated from the unscaled coordinates and velocities (x and $\dot{x}$), and the x° are the equilibrium center of mass coordinates (26). The CH local mode is scaled first so that it contains the excitation energy to within 1×10^{-5} kcal/mol. The coordinates and momenta for the remaining atoms are then scaled so that the molecule contains the excitation energy plus the ground-state energy, ensuring a microcanonical ensemble of trajectories to within 1×10^{-5} kcal/mol. The angular momentum is then recalculated and removed as necessary and the scaling procedure repeated until the system contains zero angular momentum and the energy is fixed to within 1×10^{-5} kcal/mol. The scaling procedure rarely requires more than three or four iterations.

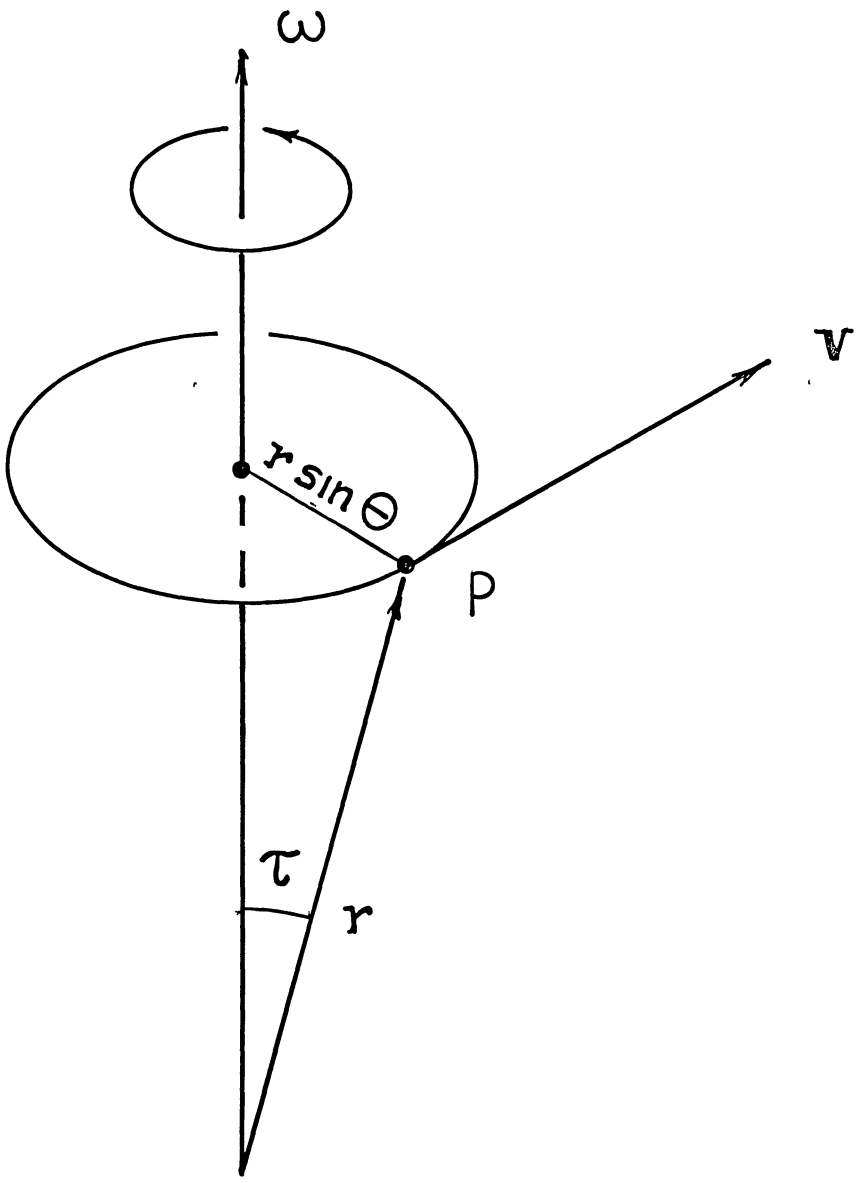

Figure 1. Linear Velocity Due to Rotation

F. Calculation of Potential Energy and Derivatives

The program is currently capable of calculating the potential energy and derivatives of the potential interactions listed in Table I. The first column of Table I lists the potential interaction "type numbers" which have been assigned to each of the interactions. The input data file, as previously described, specifies the desired number of each potential interaction type. New potential interaction terms may be incorporated into the program by adding blocks of code that calculate the desired potential and derivatives to the POTEN subroutine and by assigning an interaction "type number" to the new interaction in a manner compatible with the current program. A more complete description of the potential energy interactions is given in Chapter III.

G. Integration of the Equations of Motion

The Hamiltonian approach is used to obtain the equations of motion (30). The Hamiltonian is H = T + V where T is the kinetic energy and V is the potential energy. Hamilton's equations of motion are:

$$\begin{aligned} \frac{\partial H}{\partial p_j} &= \dot{q}_j \\ \frac{\partial H}{\partial q_j} &= -\dot{p}_j \end{aligned} \tag{26}$$

where H is the Hamiltonian, q_i are the cartesian coordinates, p_i are the conjugate momenta, and $\dot{q}_i$ and

$\dot{p}_i$ are the time derivatives of the coordinates and momenta respectively. In cartesian coordinates with the potential a function of the q_i only,

$$\frac{\partial H}{\partial p_j} = \frac{\partial T}{\partial p_j} \qquad (27)$$
$$\frac{\partial H}{\partial q_j} = \frac{\partial V}{\partial q_j}$$

The analytic derivatives of the potential with respect to the q_i are straightforward for most potential interactions. However, the analytic first derivatives of potential interaction terms involving dihedral angles and of the form shown in Equation (2) were determined as described in Section II.D. The equations of motion are integrated using a fourth-order Runge-Kutta-Gill routine. Cartesian coordinates are used for integration of the trajectories.

In the studies involving benzene, an integration stepsize of 4.89×10^{-17} s or greater was used. Energy conservation to five decimal places was obtained. Ensembles of 50 trajectories were calculated for each set of initial conditions. Preliminary results indicated that energy flow from an excited CH bond is essentially complete within .25 ps, therefore most of the trajectories were integrated for only 1 ps.

H. Final State Analysis

The analysis consists of calculation of the energy in each of the normal modes as a function of time and calculation of the CH bond energy (within the local mode

approximation) as a function of time using Equation (12). The results of the normal mode analysis of energy are purely qualitative. The normal mode description is inadequate for anything more than a rudimentary analysis of the results at the energies of interest. However, it does provide interesting insight into the mechanism by which energy transfer out of an excited CH bond occurs. It should also be noted that the validity of the normal mode analysis deteriorates significantly with trajectory time. This is evidenced by the observation that the total energy in the modes progressively deviates from the actual energy in the molecule. Calculation of the energy in each of the normal modes is accomplished by using the table of transformation coefficients, Equation (5), to transform from cartesian coordinates and momenta to normal coordinates and momenta. The following harmonic approximation is used to determine the energy in each of the normal modes:

$$V_k = \dot{Q}_k^2/2 + \lambda_k Q_k^2/2 \qquad (28)$$

where Q_k,(k=1,3N), are the normal coordinates, $\dot{Q}_k$ are the conjugate momenta, and λ_k are the respective eigenvalues.

CHAPTER III

POTENTIAL-ENERGY SURFACES

The potential-energy surfaces employed for this study of intramolecular energy transfer in benzene are written as functions of the internal coordinates. The internal coordinates include bond lengths, bond angles, CCCH out-of-plane wag angles, CCCC dihedral angles, and special coordinates which are defined as sums and differences of other internal coordinates. The CCCH wag angles are defined as the angle that a CH bond makes with the associated CCC plane with a positive angle defining movement of the H atom toward the positive z direction (31). The CCCC dihedral angles are determined as defined on page 60 of Wilson, Decius, and Cross (24). A number of the potential interaction terms used are very specific to the particular potential. Therefore, these terms were added to the energy transfer program temporarily as described in the discussion in Chapter II pertaining to code modification for specific systems.

Both anharmonic and harmonic potential-energy surfaces were used in this study. An anharmonic potential-energy surface of the form used by Nagy and Hase (32) was employed. Several potentials were used with varying

degrees of anharmonicity in order to determine the effect of anharmonicity on energy transfer. Harmonic potential-energy surfaces with varying degrees of complexity were also employed. The first harmonic potential includes no coupling terms and consists of harmonic terms for the bond lengths and bond angles only. The other two harmonic potentials are based on the ab initio and scaled potential-energy surfaces which were developed by Pulay, Fogarasi, and Boggs (31). The potentials of Pulay et al. include coupling between internal coordinates. Each of the potential-energy surfaces is described in more detail below.

The anharmonic potential (potential 1) includes Morse oscillators for the CC and CH stretches, harmonic plus quartic terms for the CCC bends, and harmonic plus quartic terms multiplied by a switching function for the CCH in-plane wags (32). The switching function attentuates the CCH in-plane wag force constants with the extension of the associated CC bonds. The form for potential 1 is:

$$V = \sum_{i=1}^{12} D_e\{1 - \exp[-\beta_i(r_i - r_i^\circ)]\}^2 + \sum_{i=1}^{6}[f^\circ_{CCC}(\theta_i - \theta_i^\circ)^2 + a^\circ_{CCC}(\theta_i - \theta_i^\circ)^4 + f_{HCC}(\alpha_i - \beta_i)^2 + a_{HCC}(\alpha_i - \beta_i)^4] \quad (29)$$

where α, β, and θ are defined as shown in Figure 2. The f and a force constants are

$$f_{HCC} = f^\circ_{HCC} S_{i,i-1} \qquad a_{HCC} = a^\circ_{HCC} S_{i,i-1} \quad (30)$$

where the switching function $S_{i,i-1}$ is given by

$$S_{i,i-1} = \exp[-w(r_{CCi} + r_{CCi-1} - 2r^{\circ}_{CC}] \quad (31)$$

The first harmonic potential (potential 2) consists of quadratic terms only for the bonds and bond angles, there are no potential energy coupling terms. Potentials 1 and 2 are only applicable to in-plane motion. There are no forces resisting movement out of the plane. The parameters for both potentials were adjusted to give acceptable agreement with the experimentally observed vibrational frequencies. Calculations were also carried out on potential 1 using parameters reported by Nagy and Hase (32,33). The potential parameters and force constants for potentials 1 and 2 are given in Table IV. Table V shows the experimental frequencies obtained by Shimanouchi (34) (as reported by Nagy and Hase (32)) and the assignments of the vibrational frequencies obtained using our anharmonic force constants for potential 1. (Our calculated frequencies are compared to the experimental frequencies of Shimanouchi (34) in order to maintain consistency with the study of Nagy and Hase (32).) Bad fits to the experimental frequencies occur primarily in bending modes. This suggests that potential 1 does not adequately describe the bending motions of the molecule. In attempting to fit these modes, large changes in the potential parameters which caused only negligible changes in the frequencies of the normal modes that involve bending (and for which bad fits were obtained) were noted, while the frequencies of the other modes deteriorated significantly. Thus, given

the limitations of the present potential form, a reasonable compromise in the fits to the normal mode frequencies has been obtained.

Potential-energy surfaces with varying degrees of anharmonicity were used to determine the influence of anharmonicity of "bath" modes on intramolecular energy transfer from a local CH stretch mode in benzene. Calculations were carried out on the surfaces to determine which "bath" modes can be treated harmonically without affecting the rate of energy transfer. All of the potentials for this part of the study are for planar benzene. Potentials 1 and 2 as described above were used for the anharmonic and purely harmonic potentials respectively. The other four potentials were obtained by using harmonic potential terms and force constants for all internal coordinates except for the terms listed in the second column of Table VI. The anharmonic and harmonic potential parameters are given in Table IV.

Potentials 7 and 8 are harmonic potentials with coupling terms based on the ab initio and scaled potential-energy surfaces of Pulay et al. (31) respectively. Potential terms with small force constants were neglected in order to reduce the computation time. Only potential terms with force constants on the order of 15 (see Table VII for explanation of units) and larger were included from the Pulay et al. potentials, and no coupling terms involving out-of-plane motions were included. In order to

determine the effect of out-of-plane motions on energy decay from an excited CH bond, calculations including out-of-plane motions were carried out on potential 8. The potential-energy terms and force constants are given in Table VII. The scaled planar potential differs from the potential shown in Table VII only in that the out-of-plane force constants are set equal to zero. Exclusion of potential interaction terms with small force constants resulted in deviation of the frequencies shown in Table VIII, which were calculated from the potentials shown in Table VII, from those reported by Pulay et al. (see Table IX, Reference 31). As noted by Ozkabak, Goodman, Thakur, and Krogh-Jespersen (35), exclusion of even the smallest force constants causes shifts in the calculated frequencies. However, a model of benzene is obtained which predicts reasonable normal mode frequencies. Concern about neglecting potential-energy coupling terms between the CH stretch and CCH wag might be justified since previous studies indicate that resonance interactions between these modes are responsible for the rapid relaxation of energy from the CH stretch mode (1,2,5,6,7,8). However, the force constants for interactions which explicitly couple these modes are an order of magnitude smaller than the smallest term included in the potential.

Potentials 7 and 8 include coupling terms for the CH bonds in addition to the harmonic term. Therefore a harmonic approximation, Equation (12), was employed in the

assignment of the initial excitation energy to one of the CH bonds and to calculate the energy in each of the CH bonds as a function of time.

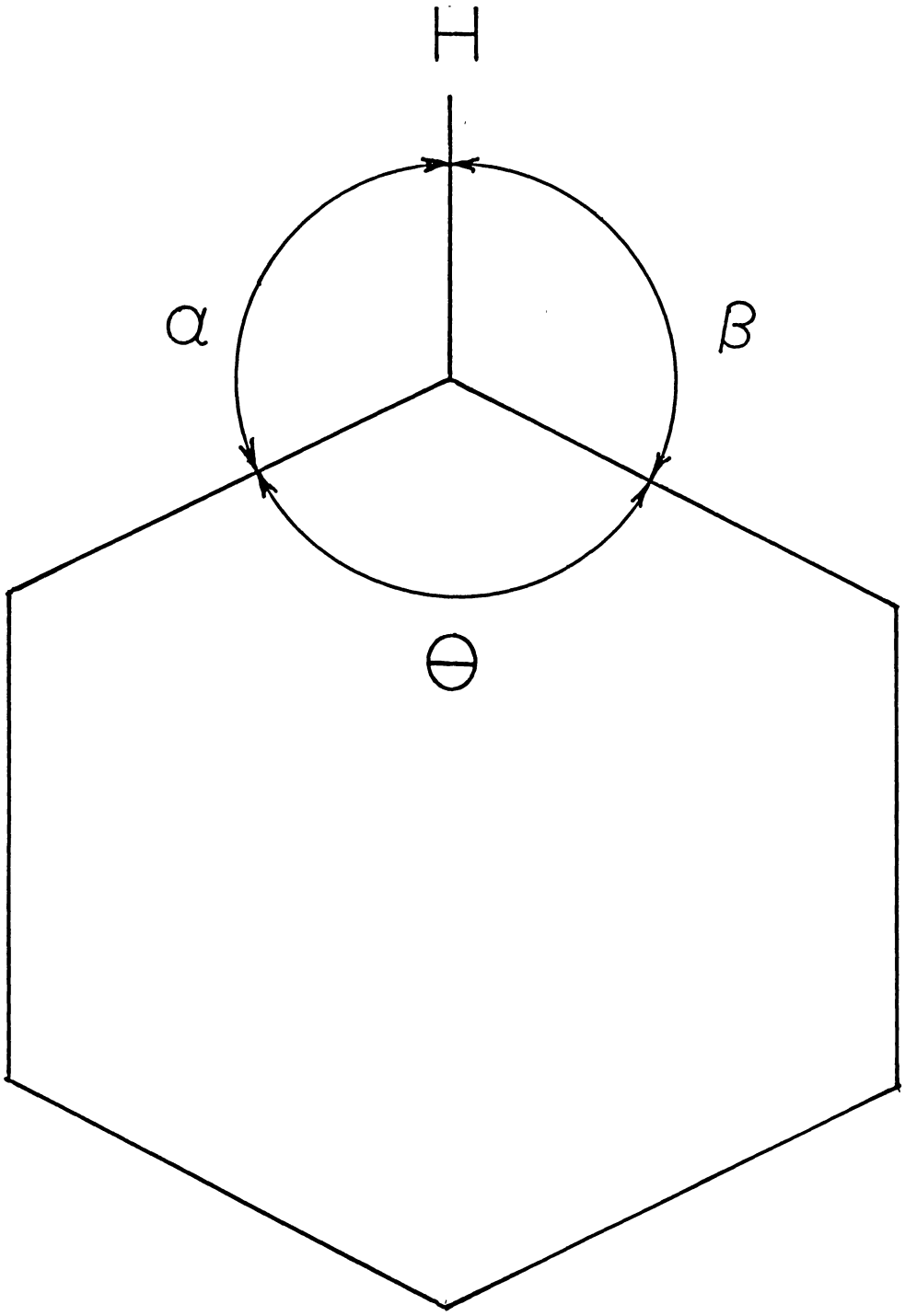

Figure 2. Definition of Angles for Potential 1

TABLE IV

PARAMETERS: POTENTIALS 1-2

Anharmonic Potential

Morse Functions:

Bond	D_e	$\beta(A^{-1})$	$R_e(A^o)$
C-H	105.0	1.870	1.080
C-C	130.0	2.054	1.390

Bending Constants:

Angle	f_o(kcal/mol·rad^2)	a_o(kcal/mol·rad^2)
CCC bend	181.000	7.250
CCH wag	34.650	1.386

Harmonic Potential

Force Constants:

bond	k(kcal/mol·A^2)	$r_o(A^o)$
C-H	732.400	1.080
C-C	1097.000	1.390

Bending Constants:

Angle	k(kcal/mol·rad^2)	θ^o(degrees)
CCC bend	152.000	120
CCH wag	56.000	120

TABLE V

FREQUENCIES: POTENTIAL 1

Mode[a]	Symmetry	Frequency (cm^{-1})	
		Calculated	Experimental[b]
1	A_{1g}	3066	3062
2	A_{1g}	992	992
3	A_{2g}	1326	1326
4	A_{2u}[c]		
5	B_{1u}	3067	3068
6	B_{1u}	1004	1010
7	B_{2g}[c]		
8	B_{2g}[c]		
9	B_{2u}	1144	1310
10	B_{2u}	1852	1150
11	E_{1g}[c]		
12	E_{1u}	3066	3063
13	E_{1u}	1010	1486
14	E_{1u}	1538	1038
15	E_{2g}	3067	3047
16	E_{2g}	1114	1596
17	E_{2g}	1808	1178
18	E_{2g}	610	606
19	E_{2u}[c]		
20	E_{2u}[c]		

(a) G. Herzberg, Molecular Spectra and Molecular Structure. II. Infrared and Raman Spectra of Polyatomic Molecules (van Nostrand Reinhold, New York 1945), p. 118.

(b) T. Shimanouchi, Ref. 34.

(c) Out-of-plane modes.

TABLE VI

POTENTIALS 3-6

Potential	Anharmonic Terms
3	1 CH stretch
4	1 CH stretch, 1 CCCH wag
5	6 CH stretches
6	6 CH stretches, 1 CCCH wag

TABLE VII

POTENTIAL PARAMETERS[a,b]

Potential Term	*Ab Initio* Force Constants	Scaled Force Constants
$r_1^2/2$	829.0079	744.8264
$r_1 q_{19}$	-18.2753	-15.1095
$r_1 q_{20a}$	-17.2680	-14.2461
$R_1^2/2$	1027.0143	954.9204
$R_1 R_2$(o)	131.9563	91.0887
$R_1 R_3$(m)	-92.2399	-63.6038
$R_1 R_4$(p)	91.8082	63.3160
$R_1 \beta_1$	28.2044	24.0313
$R_1 q_{20a}$	22.5923	19.2826
$\beta_1^2/2$	92.0960	73.6768
$q_{19}^2/2$	222.9011	177.8604
$q_{20a}^2/2$	222.7572	177.8604
$\gamma_1^2/2$		63.1577
$q_{28}^2/2$		54.1496
$q_{29a}^2/2$		45.4148

[a]See Pulay *et al.*, Ref. 31, for definition of potential terms.

[b]Energy units are kcal/mol; coordinate units are angstroms and radians.

TABLE VIII

FREQUENCIES

Symmetry Type	Frequency (cm^{-1})		
		Calculated	
	Experimental[a]	Scaled Force Constants	*Ab Initio* Force Constants
A_{1g}	3073	3087	3257
	993	953	1010
A_{2g}	1350	1382	1540
B_{1u}	3057	3057	3224
	1010	995	1114
B_{2u}	1309	1455	1502
	1146	1090	1080
E_{1u}	3064	3085	3255
	1482	1531	1676
	1037	967	1039
E_{2g}	3056	3075	3244
	1599	1780	1907
	1178	1128	1245
	606	719	794

[a]Experimental frequencies are from Ref. 36.

CHAPTER IV

RESULTS AND DISCUSSION

The purpose of this study is to investigate the rates and mechanisms of intramolecular energy transfer in large molecules. The results reported here are for benzene which has already been the focus of several studies. The influence of initial conditions and potential on the rate of energy flow out of an excited CH stretch local mode of benzene has been investigated. The effect of anharmonicity was explored by the use of harmonic and anharmonic potential-energy surfaces and by the use of potential-energy surfaces with varying degrees of anharmonicity. Models have been employed which restrict atomic motions to the molecular plane with the exception of one model which was used to determine the effect of out-of-plane motion on the energy transfer results. The potential-energy surfaces are described in detail in Chapter III.

In examination of the plots shown in this study, it should be noted that slight deviations in the structures of similar plots might be attributed in part to statistical error.

Figures 3 and 4 show the results for initial CH excitation of 50 and 71.5 kcal/mol, respectively; these are

plots of the CH energy as a function of time, computed using the anharmonic potential, potential 1. As described in Chapter II, the initial conditions were obtained by assigning zero-point energy to all the normal modes (a total of 52.69 kcal/mol) and the excitation energy to the CH stretch. Rapid and irreversible loss of energy by the CH stretch is observed at both excitation energies. This is in qualitative agreement with the results obtained by Sibert et al. (see Figure 2 of Reference 5). The dynamics were not analyzed to determine an explanation for the rapid energy transfer that was observed. However, it can be inferred from the good agreement with the model studies of Sibert et al. (5) that the Fermi resonance between the CH stretch and CCH wag modes facilitates the flow of energy out of the excited CH bond. The rate of energy transfer is approximately the same for both CH excitation energies. Approximately 42 percent of the initial energy has drained out of the CH stretch within .1 ps. The CH energy rapidly reaches a constant value of approximately 13 percent of the initial value. It is interesting that the results are essentially the same for the two initial excitations shown in Figures 3 and 4 (50 and 71.5 kcal/mol, respectively). There are some minor differences in the details of the two plots, but these can probably be discounted because of the small ensemble size. These results are in contrast to those obtained by Nagy and Hase (32), however, as they have pointed out, the CCH force constant used in their

calculations was too large (33). Using 1090.76 kcal/mol rad^2 for the CCH force constant, they found no energy transfer out of the CH stretch in 2 ps. The results of this study, Figures 3 and 4, for a more realistic value of the constants, give very rapid energy flow from the local mode.

As noted, these results are similar to those reported by Sibert et al. (5). They followed the trajectories for only 0.2 ps. Thus, comparison to their results can only be made with the initial portions of the curves in Figures 3 and 4. There are some minor differences in the short-time region of the results of this study and the plots reported by Sibert et al. (see Figure 2 of Reference 5). The results shown in Figures 3 and 4 appear to display somewhat slower decay of the CH excitation energy than do theirs. Nevertheless, the agreement is satisfactory considering the differences in the two models.

Figure 5 shows a plot of the energy flow from the excited bond as a function of time for initial CH excitation of 50 kcal/mol calculated using a harmonic potential, potential 2. In addition to the CH excitation energy, the normal modes are initially assigned zero-point energy. This result is qualitatively different from that obtained using the anharmonic potential, potential 1, which is shown in Figure 3. Energy transfer out of the initially excited CH bond occurs much less rapidly than for the anharmonic potential. The energy transfer for the harmonic

potential (Figure 5) occurs in two stages--initially there is a very rapid loss by the CH stretch followed by a rather gradual flow of energy from the bond that continues up to about one picosecond, while in the anharmonic case (Figure 3) the net loss of CH stretch energy is complete within less than a half of a picosecond. Obviously, the anharmonicity significantly facilitates the energy flow from the CH bond to the rest of the molecule.

Figure 6 shows a plot of the energy as a function of time for one of the initially unexcited CH stretches (the para position, in this case) for initial CH excitation of 50 kcal/mol using potential 1 (see Figure 3) with zero-point energies in all the normal modes. There is a delay time of about 0.2 ps before energy flows into the bond. Once the energy begins to enter the stretch it rapidly increases, then decreases until it levels out at about 0.4 ps. At 2 ps all six CH stretches contain approximately the same amount of energy, roughly eight kcal/mol. The results for the ortho and meta CH stretches are similar to those for the para shown in Figure 6, i.e., the energy appears to transfer into the bonds at about the same time; however, the magnitude of the initial energy transfer into the ortho and meta positions appears to be somewhat less than in the para case. Similar but more pronounced results were obtained for the higher energy (71.5 kcal/mol CH initial excitation) and for the harmonic case at the same energy (50 kcal/mol CH initial excitation) as shown in Figures 7

and 8, respectively.

Calculations were also performed with potential 1 using the two sets of potential parameters reported by Nagy and Hase (32,33). The results of these calculations are shown in Figures 9 and 10. The initial conditions are the same as those used by Hagy and Hase (see Figure 2, Case I, of Reference 32), that is 50 kcal/mol in one CH stretch and no energy in the rest of the molecule. The results in Figure 9 are for the potential parameters given in Table I of Reference 32. The calculations (Figure 9) using the Nagy-Hase potential (32) show an initial rapid loss of energy by the CH stretch, half of which is reversible up to about 1 ps. After 1 ps, there is still some "structure" in the plot, but it damps out as the time increases. These results appear to be due to the large value of the CCH in-plane wag force constant. Calculations performed with the same initial conditions, that is, all of the energy initially in one CH stretch, using the anharmonic potential parameters in Table IV, show no energy transfer out of the initially excited CH bond. A series of calculations, using ensembles of 30 trajectories, which differed only in the value of the CCH wag force constant indicate that energy transfer out of the initially excited CH stretch increases as the CCH wag force constant is increased up to a value of approximately 130 kcal/mol rad^2. Beyond this value, no energy transfer is observed using these initial conditions. Figure 10 shows the results obtained using the Nagy-Hase

potential reported in Reference 33. The initial conditions are the same as those for the calculations just discussed (and used by Nagy and Hase). In this case no energy transfer is observed, in agreement with the results of Nagy and Hase (32). These results also display the dependence of the rate of energy transfer from the excited CH bond upon the force constant of the associated CCH wag and hence upon the vibrational frequency of the CCH wag. This demonstrates the importance of resonance interactions in the energy transfer mechanism.

In order to investigate the influence of anharmonicity of the various modes of benzene on the energy transfer from an excited local CH stretch mode, calculations were carried out employing potential-energy surfaces with varying degrees of anharmonicity (potentials 3-6). Calculations were carried out for two energies, 50 and 71.5 kcal/mol CH stretch excitations; the zero-point energy assigned to the normal modes amounts to 51.55 kcal/mol. Four different versions of the valence-force potential-energy surface were investigated (potentials 3-6, see Table VI) in addition to potentials 1 and 2 discussed above. Potentials 1-6 are all restricted to planar benzene. The results of potential 1 as compared to potential 2 as already discussed show that the fully harmonic potential (potential 2) is a poor approximation to the more realistic anharmonic potential. The purpose of the calculations involving potentials 3-6 is to investigate the intermediate cases.

Ensembles of 50 trajectories were integrated for 0.5 ps. While the energy transfer out of the CH bond is not always complete within this time, it is nearly so. In the calculations involving potentials 1 and 2, discussed above, integrations were carried out to 2 ps. It is clear on the basis of those results that 0.5 ps is sufficient time to determine the nature of the energy transfer to answer the question addressed here, namely the effect of anharmonicity on the energy transfer from an excited CH stretch local mode in benzene.

Results for potentials with varying degrees of anharmonicity are shown in Figures 11 and 12. Those in Figure 11 are for 50 kcal/mol excitation and those in Figure 12 for 71.5 kcal/mol. The results in Figure 11 can be compared with those in Figure 3 and Figure 5 for the fully anharmonic and harmonic potentials since thay are for the same total energies. If the stretch potential for the excited CH bond is represented by a Morse potential while the rest of the molecule is treated harmonically (potential 3), the rate of energy transfer is significantly faster than in the harmonic case as can be seen by comparing the plot in Figure 11a (one anharmonic bond) with that in Figure 5 (fully harmonic). The energy transfer curve for the case of one anharmonic bond is qualitatively similar to that for the totally harmonic potential in that there is an initial rapid loss followed by a slower decay of the CH stretch energy. These results show that the single

anharmonic bond potential is a much better approximation than the totally harmonic potential. The rate of energy transfer is further increased by making the HCCC in-plane wag associated with the excited bond anharmonic (potential 4) as shown by the plot in Figure 11b. Similar results are observed for 71.5 kcal/mol excitation energy as shown by Figures 12a and 12b.

It is clear from these results that it is an excellent approximation to treat the molecule harmonically if the excited mode (CH stretch) and the associated CCCH in-plane wag potential include anharmonicity.

These results invited further investigation to see if introducing anharmonicity into other modes has an effect on the energy transfer. The results in Figures 12c and 12d show results for potentials 5 (six anharmonic CH stretches) and 6 (six anharmonic CH stretches plus one anharmonic wag). These results show that adding anharmonicity to the initially unexcited CH stretches has essentially no effect on the energy transfer rate. Based on these results, it can be inferred that there would be no change in the energy transfer rate upon introduction of anharmonic terms for the CC stretches.

As demonstrated from the results obtained with potentials 1-6, it appears to be essential that the modes which are intricately involved in the energy transfer process be treated anharmonically (e.g. the CH stretch and CCH in-plane wag modes in benzene). However, further

investigations of energy transfer in benzene using potentials 7 and 8 indicate that the form of the potential energy surface can also play an important role in the energy transfer results. Potential-energy coupling terms are present in potentials 7 and 8 which are absent in potentials 1-6. While explicit coupling terms between the CH bond and the CCH wag modes are not included (the force constants for these interactions are an order of magnitude smaller than the smallest term included in the potentials, see Table VII), there is explicit coupling between the CH bonds and the CCC angles and between the CC bonds and the CCH wag angles. Although no definitive mechanism has been investigated to determine the actual pathway through which energy transfer occurs, it appears that these secondary coupling terms contribute significantly to the energy transfer process.

The planar normal-mode frequencies calculated using forms of both the ab initio (potential 7) and scaled (potential 8) potentials are shown in Table VIII. Experimental frequencies are also shown for comparison (36). Results are included for both planar and nonplanar forms of potential 8. A normal mode analysis was used to follow the flow of energy out of the excited CH bond. The results of this analysis are purely qualitative. The normal mode description is inadequate for anything more than a rudimentary analysis of the results at the energies of interest. However, it does provide interesting insight

into the mechanism by which energy transfer out of an excited CH bond occurs. It should also be noted that the validity of the normal mode analysis deteriorates significantly with trajectory time. This is evidenced by the observation that the total energy in the modes progressively deviates from the actual energy in the molecule.

The scaled force constants shown in Table VII were used in the calculation for which the normal mode analysis of energy transfer from an excited CH stretch in benzene was obtained. The frequencies that were calculated using the scaled force constants are presented by symmetry type in Table VIII. Figure 13 shows energy flow into representative planar normal-modes. The initial excitation energy for one CH bond was 50 kcal/mol with the rest of the molecule containing ground-state energy. As shown in Figure 13a for one of the E_{2g} modes (calculated frequency = 719 cm^{-1}), there is no significant flow of energy into the lower frequency normal modes. This behavior is observed for modes with calculated frequencies as high as 995 cm^{-1}. Plots of energy flow into modes with calculated frequencies in the range from 1090 to 1231 cm^{-1} show slightly more structure than do the lower frequency modes. However, as shown in Figure 13b for another E_{2g} mode (calculated frequency = 1128 cm^{-1}), there is still no significant energy flow into these modes. The A_{2g} mode (calculated frequency = 1381 cm^{-1}) is shown in Figure 13c. Energy flow

into this mode is rapid, occurring in less than 0.2 ps. Similar behavior is observed for modes with calculated frequencies in the range of 1381 to 1780 cm^{-1}. Within this range of frequencies, the modes into which energy is flowing most rapidly are those which appear to possess the most CCH bend character such as the E_{1u} mode (calculated frequency = 1531 cm^{-1}) shown in Figure 13d. Energy flow into the mode again occurs in less than 0.2 ps. Energy rapidly decays from the mode, leveling off at approximately .25 ps and then decaying further around 1 ps. The magnitude of energy flow into the E_{1u} mode is significantly enhanced relative to the A_{2g} mode shown in Figure 13c indicating that the higher frequency E_{1u} mode is more strongly coupled to the excited CH stretch mode although both modes possess significant CCH wag character. Energy flows somewhat slower into modes in the frequency range of 1381 to 1780 cm^{-1} which appear to possess more ring stretch character as shown in Figure 13e (calculated frequency = 1780 cm^{-1}) for an E_{2g} mode. This suggests that energy may be decaying from the CH stretch mode into modes with CCH bend character and then from the bending modes into ring bath modes. However, some of the modes initially involved in the transfer of energy from the CH stretch mode include ring stretch and deform character as well as CCH bend character. The higher frequency modes (3057 to 3087 cm^{-1}) are activated by excitation of the local CH mode. The decay of energy from these modes is rapid and essentially

irreversible as shown in Figure 13f for the A_{1g} symmetric stretch mode (calculated frequency = 3087 cm^{-1}). As previously noted, a normal mode analysis cannot be considered to be quantitatively accurate for finite displacements. However, the results are in qualitative agreement with the theoretical studies of Sibert et al. (5) which indicate that a resonance between the CH stretch and the in-plane CCH bend modes is instrumental in enhancing the rate of energy flow out of the CH bond. Energy appears to be rapidly flowing into the modes with CCH wag character. The energy then decays from these modes into bath modes with frequencies in a range such that resonance interactions might be expected. The modes which possess CH stretch character are activated by excitation of the CH bond. Energy decays rapidly from these modes with little or no reversibility. The results also predict the existence of two sets of bath modes as suggested by Stannard and Gelbart (9). The low frequency modes do not participate significantly in the dispersal of energy from the excited CH stretch mode. The higher frequency modes (calculated frequencies in the range of 1381 to 1780 cm^{-1}) with which resonance interactions might occur appear to be strongly coupled to the excited CH stretch mode and actively participate in the energy redistribution process.

Figure 14 shows energy flow from a local CH stretch mode with an initial excitation energy of 50 kcal/mol. These results were obtained employing only planar potential

terms with force constants greater than 15 (see Table VII for units) from the ab initio Pulay et al. (31) potential (potential 7). In agreement with the results obtained for the planar anharmonic potential, potential 1, energy transfer out of the CH bond is rapid however there is some reversibility following the initial rapid decay of energy from the bond. The calculation was repeated using an initial excitation energy of 71.5 kcal/mol in one of the CH bonds. The results, shown in Figure 15, are essentially in agreement with the lower energy results, however, there is slightly more reversibility observed and the energy flow damps out slightly faster than for the 50 kcal/mol excitation. Figures 16 and 17 show energy flow from CH bonds containing initial excitation energies of 50 and 71.5 kcal/mol respectively. The potential is as described for Figures 14 and 15 except the scaled force constants were employed (potential 8). Two notable differences were observed using the scaled force constants. As shown in Figures 16 and 17, there is essentially no reversibility of energy flow in the bonds at either excitation energy. Enhanced flow of energy into the CH bond para to the initially excited CH bond was noted as indicated in Figures 18 and 19 for 50 and 71.5 kcal/mol of initial excitation energy respectively. This enhancement was not observed when the ab initio force constants were used (potential 7).

Figure 20 shows energy flow from a CH bond which initially contained 71.5 kcal/mol of excitation energy. A

form of the Pulay *et al.* (31) potential was employed which incorporated out-of-plane as well as planar terms with scaled force constants greater than 15 from potential 8 (see Table VII for units). The initial conditions do not include dihedral terms, however torsional motion was allowed in the dynamics. Rapid energy flow is again observed with very little reversibility. As shown in Figure 21, energy flow into the para position was significantly enhanced. However, there is no notable difference in these results relative to those obtained using the planar form of potential 8 which indicates that the out-of-plane motions do not contribute significantly to the rate of energy flow from an excited CH bond in benzene.

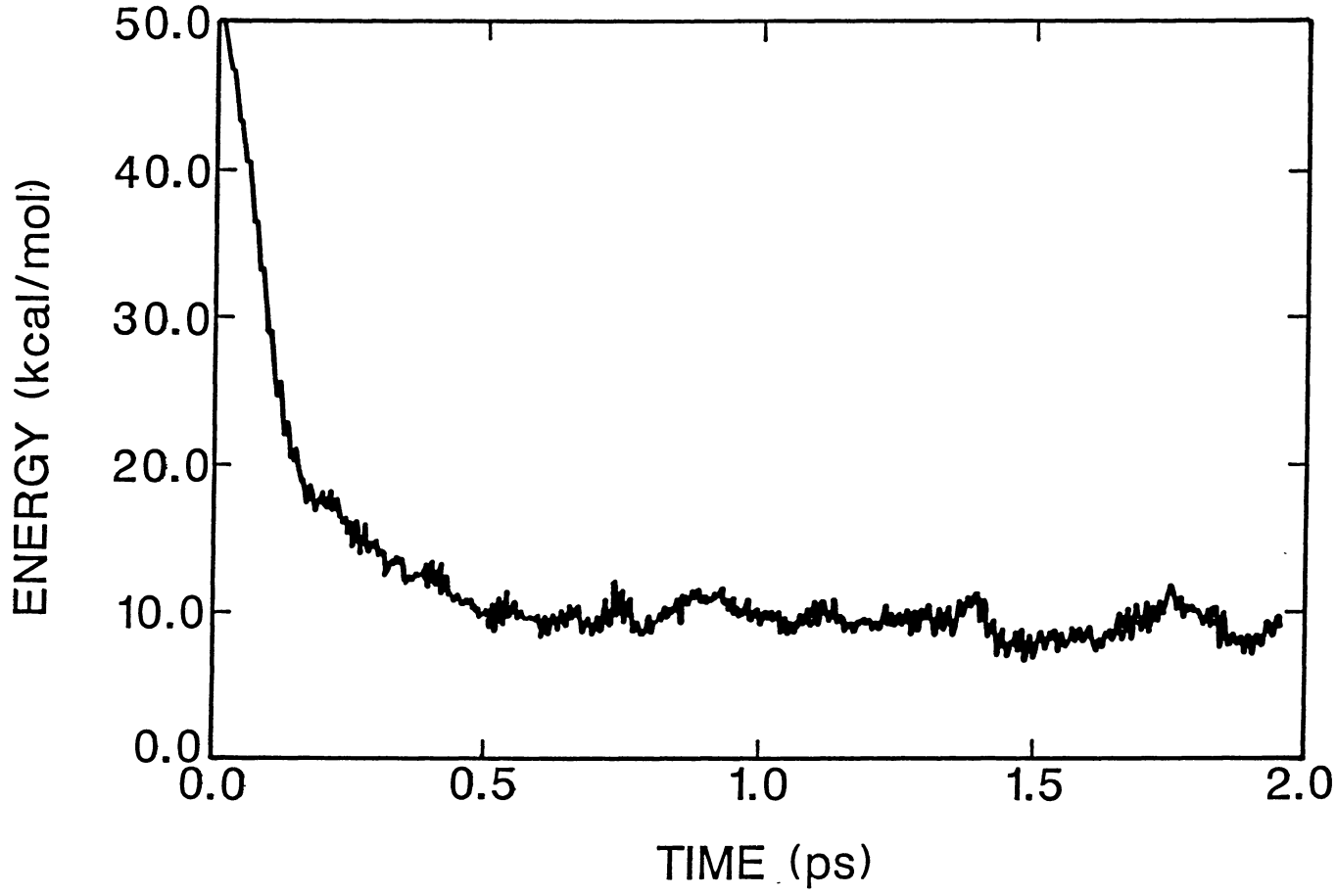

Figure 3. A plot of the average energy in the initially excited C-H stretch as a function of time for an ensemble of 50 trajectories. The anharmonic potential is described in Table IV.

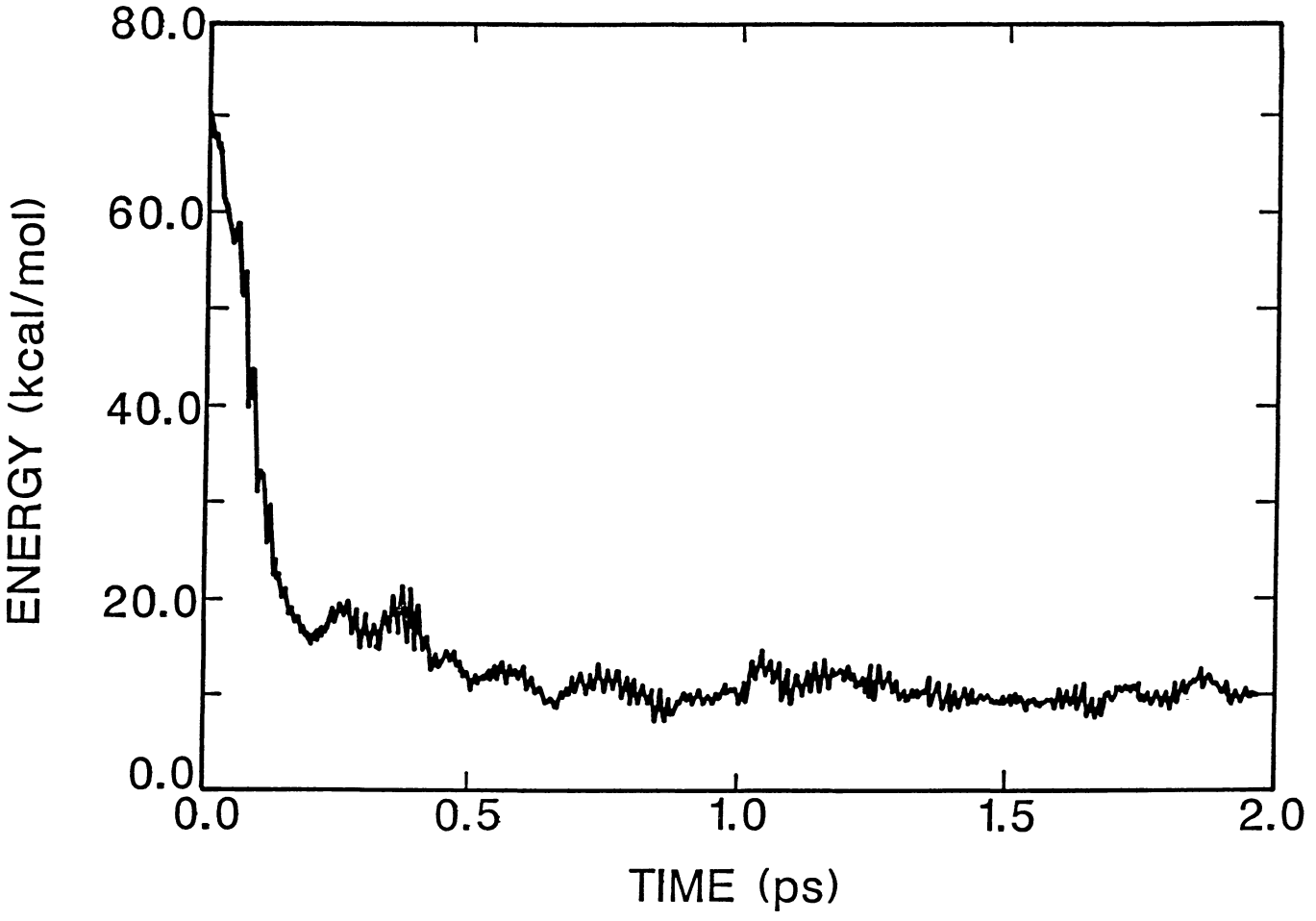

Figure 4. Same as Figure 3 except the initial C-H excitation energy is 71.5 kcal/mol.

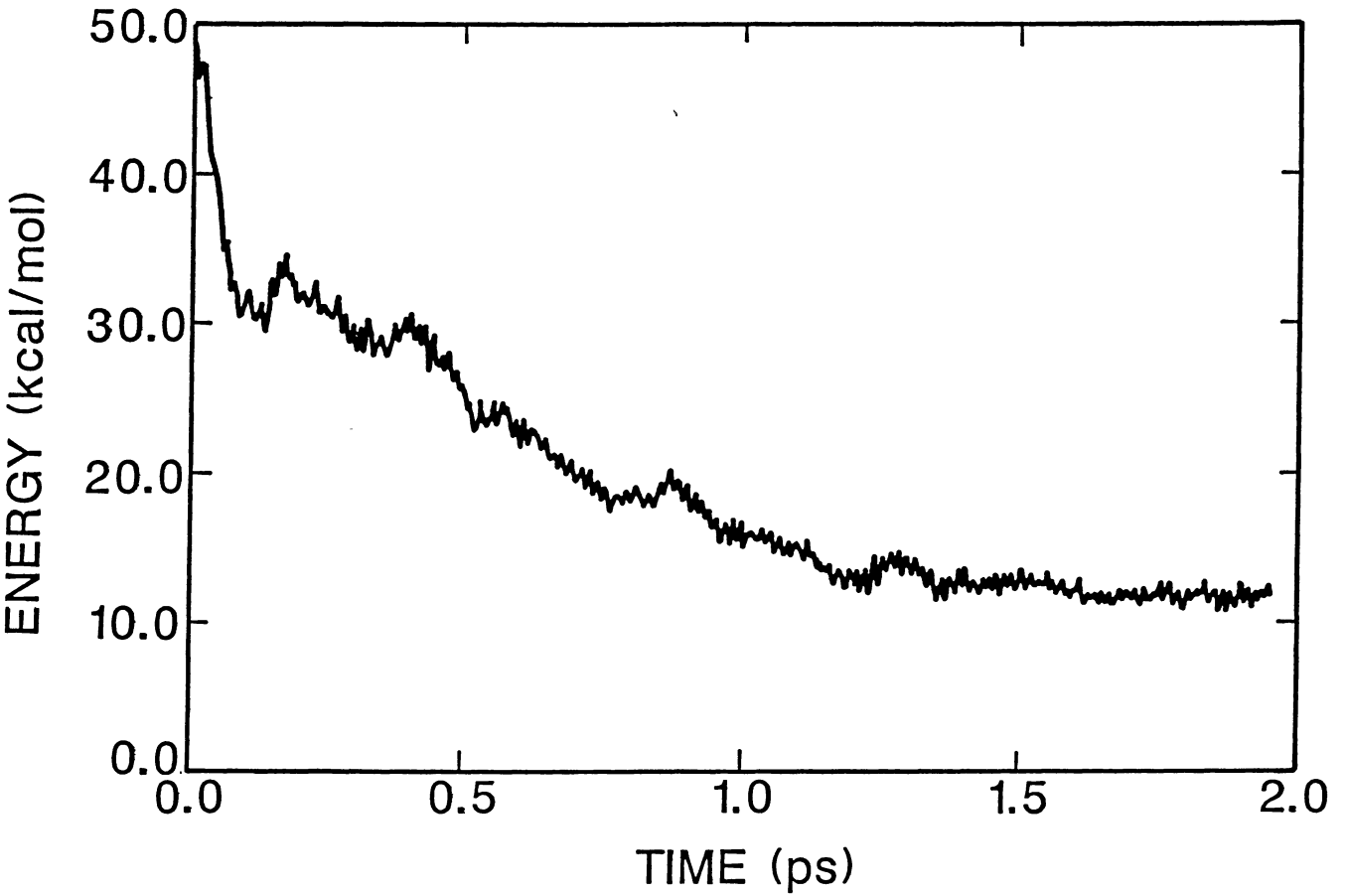

Figure 5. Same as Figure 3 except the potential is harmonic (described in Table IV).

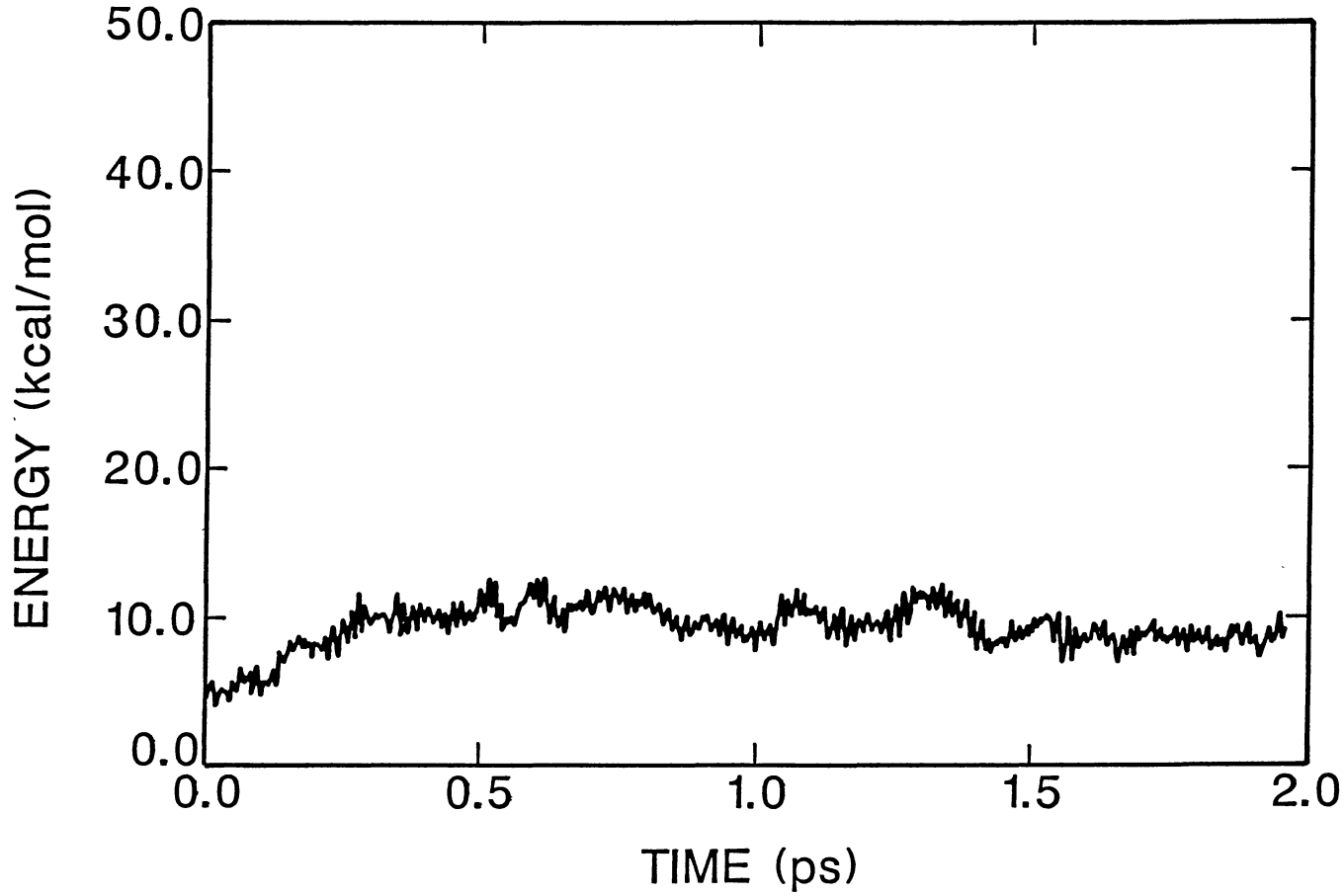

Figure 6. A plot of the average energy in the C-H bond para to the initially excited C-H bond as a function of time for the same ensemble of trajectories in Figure 3.

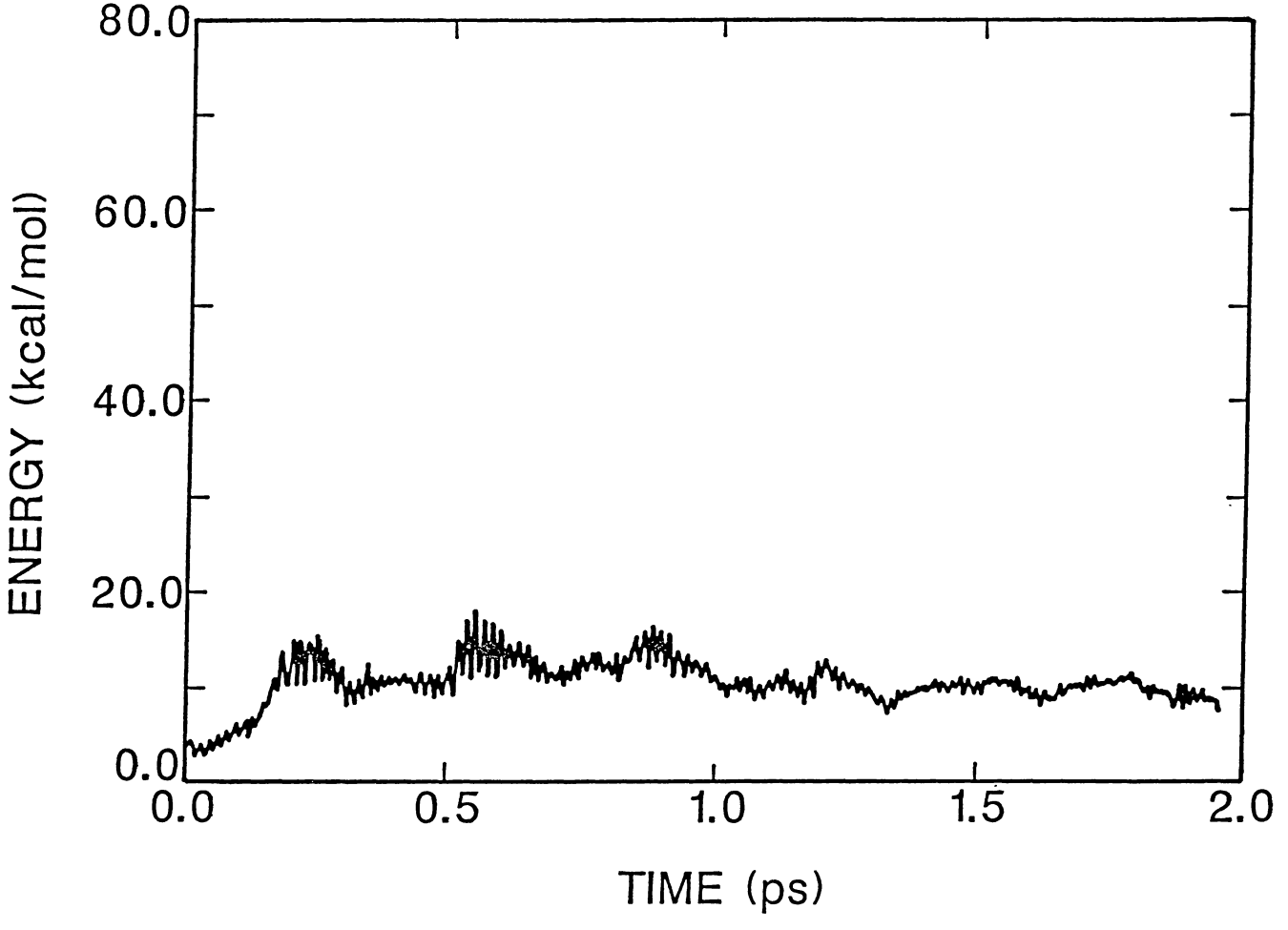

Figure 7. A plot of the average energy in the C-H bond para to the initially excited C-H bond as a function of time for the same ensemble of trajectories in Figure 4.

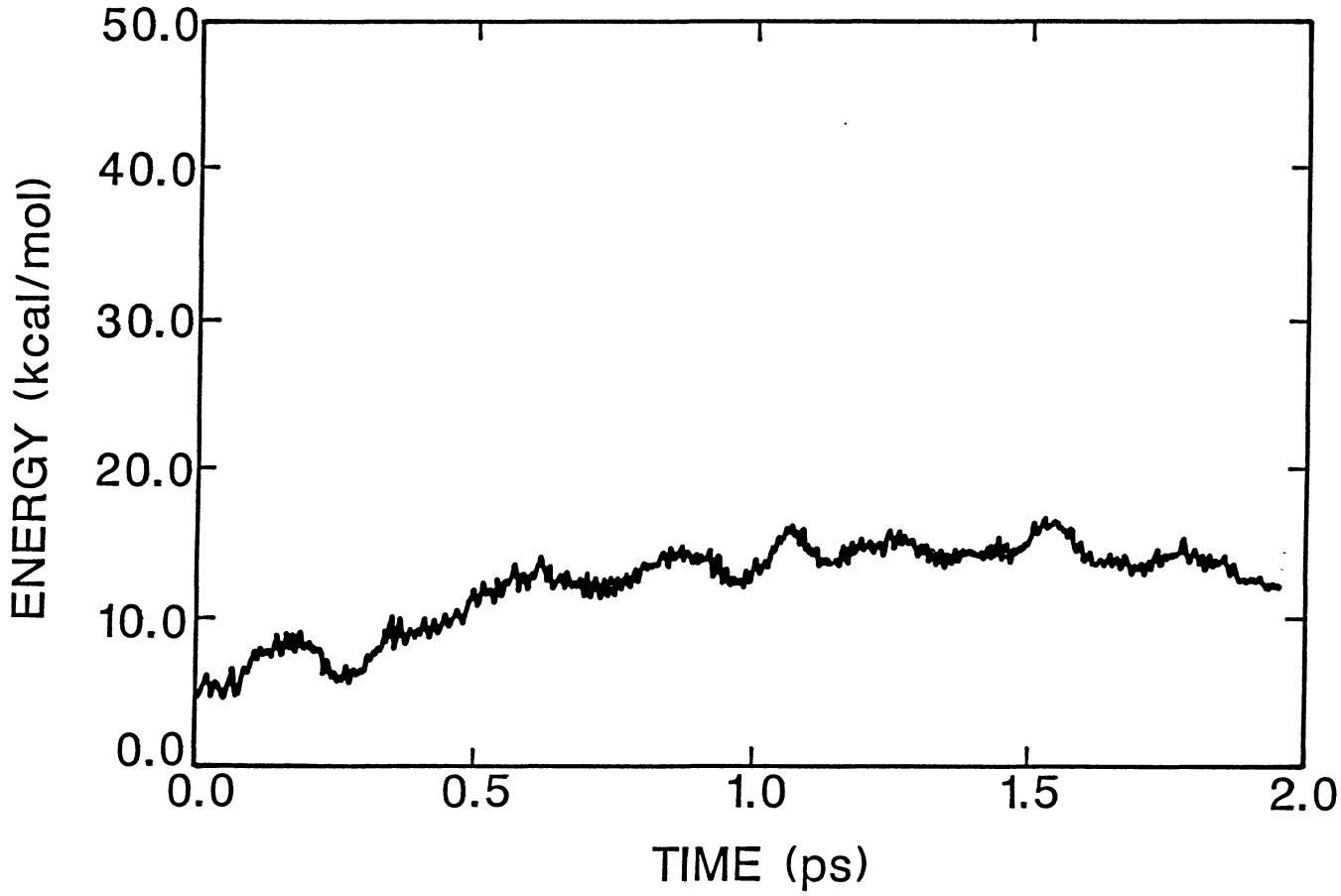

Figure 8. A plot of the average energy in the C-H bond para to the initially excited C-H bond as a function of time for the same ensemble of trajectories in Figure 5.

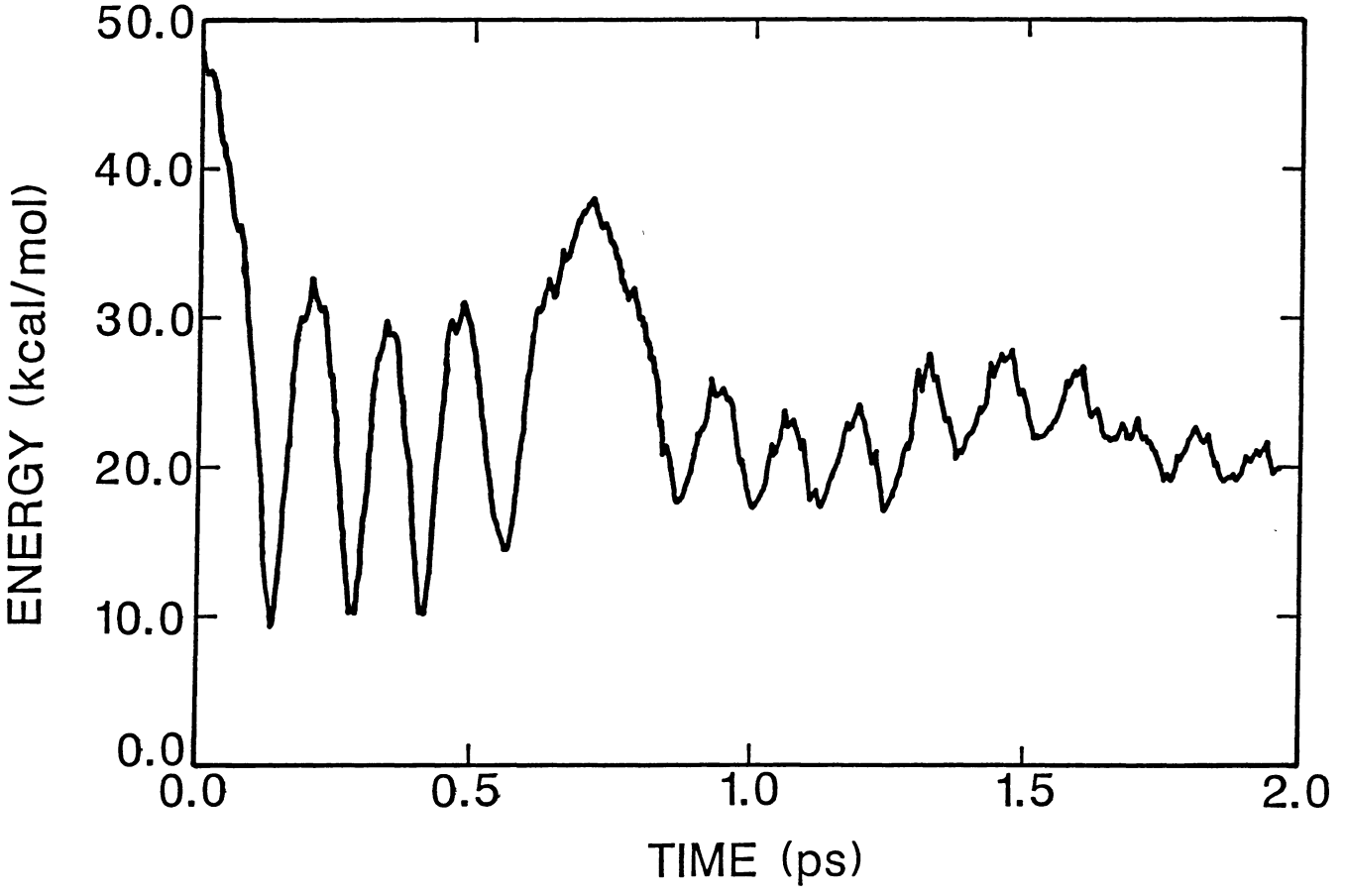

Figure 9. A plot of the average energy in the initially excited C-H stretch as a function of time for an ensemble of 50 trajectories. The potential is that reported by Nagy and Hase, see Table I of Reference 32.

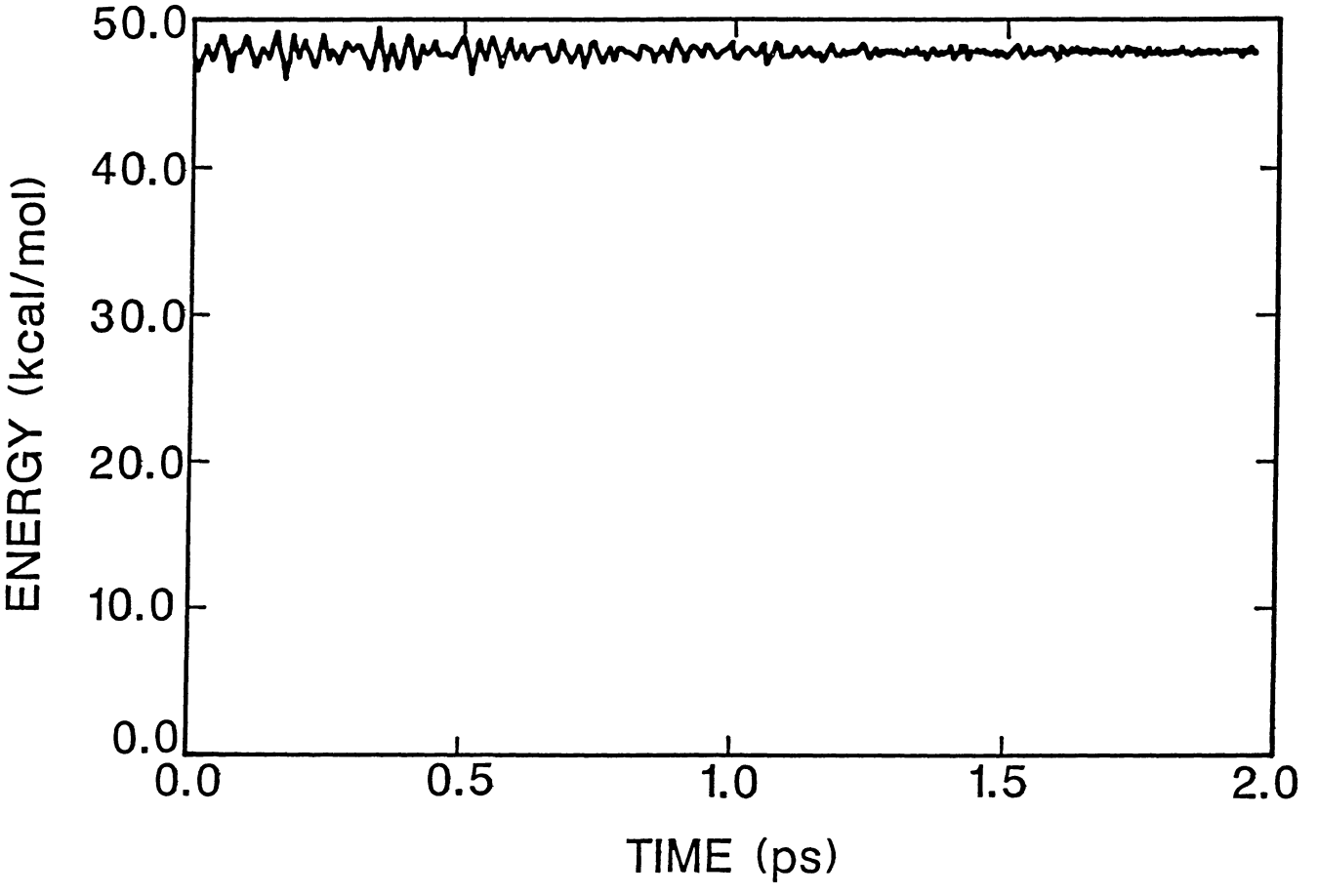

Figure 10. Same as Figure 9 except the potential is that reported by Nagy and Hase in Reference 33.

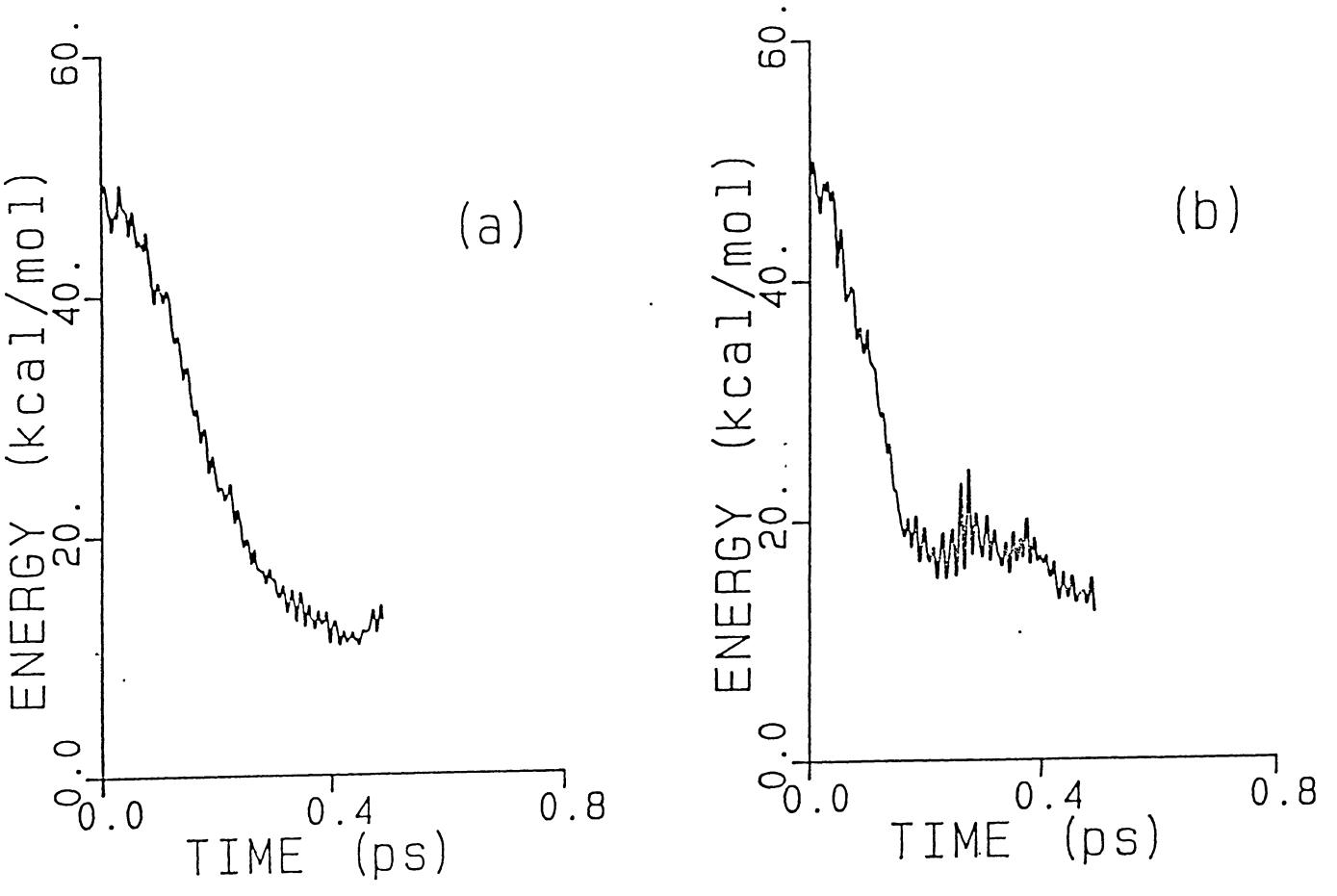

Figure 11. Average energy flow out of a C-H stretch for an ensemble of 50 trajectories. The initial C-H local mode excitation is 50 kcal/mol. The zero-point vibrational energy is 51.55 kcal/mol.
(a) One CH stretch anharmonic, potential 3;
(b) One CH stretch and one wag anharmonic, potential 4.

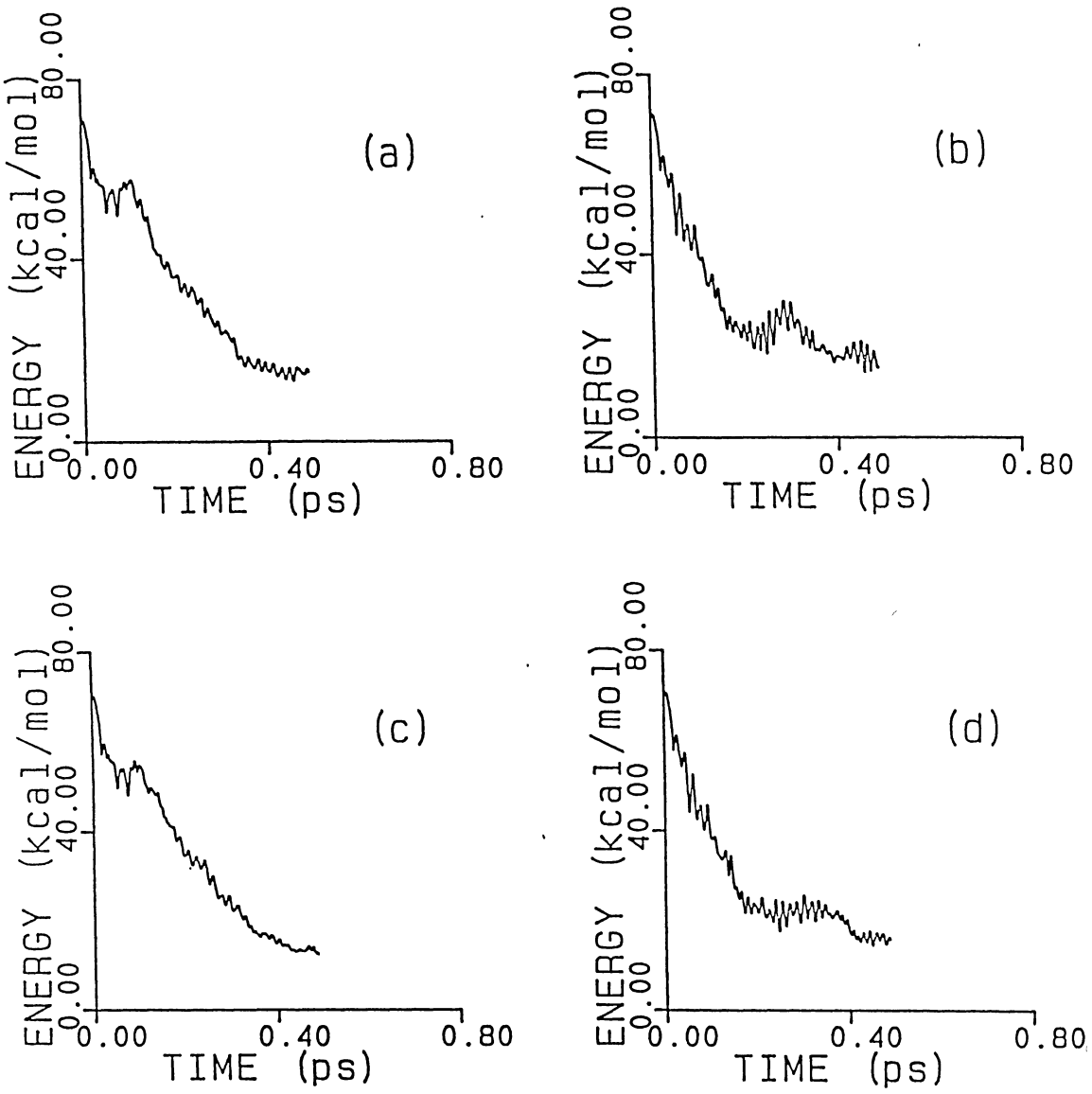

Figure 12. Same as Figure 11 except: The initial CH local mode excitation is 71.5 kcal/mol. (a) Potential 3; (b) Potential 4; (c) Potential 5; (d) Potential 6.

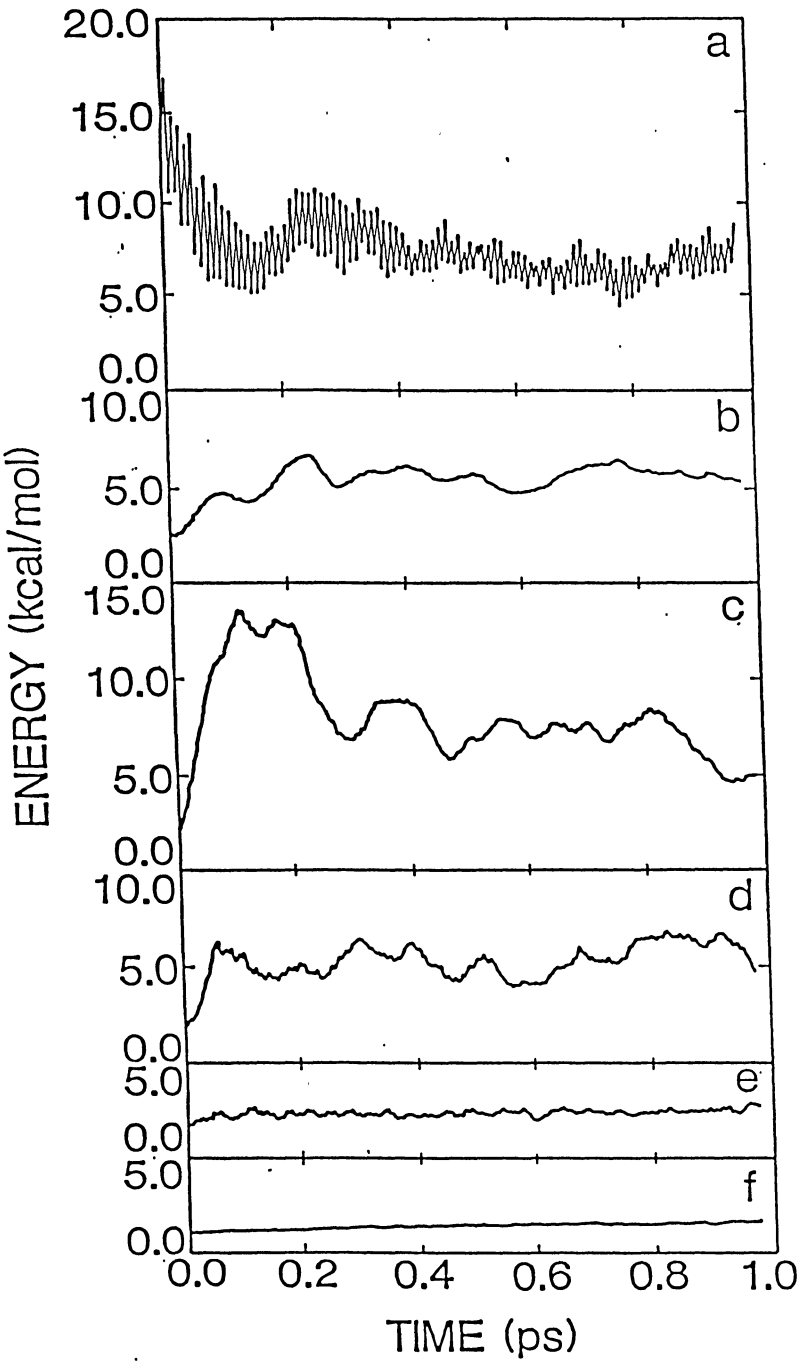

Figure 13. Plots of the average energy in representative normal-modes of benzene as a function of time for an ensemble of 50 trajectories.

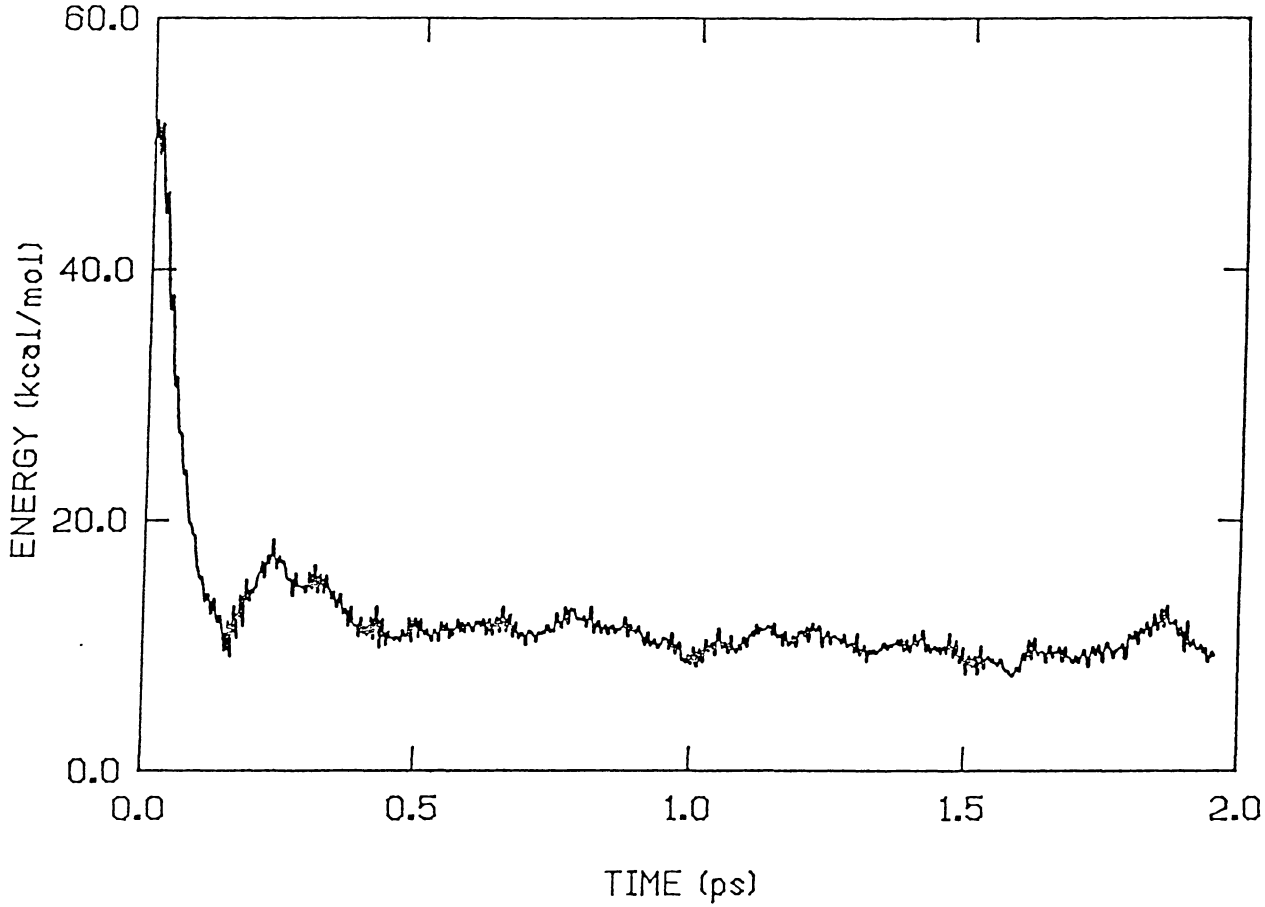

Figure 14. A plot of the average energy in the initially excited CH stretch as a function of time for an ensemble of 50 trajectories. The ab initio force constants shown in Table VII were used.

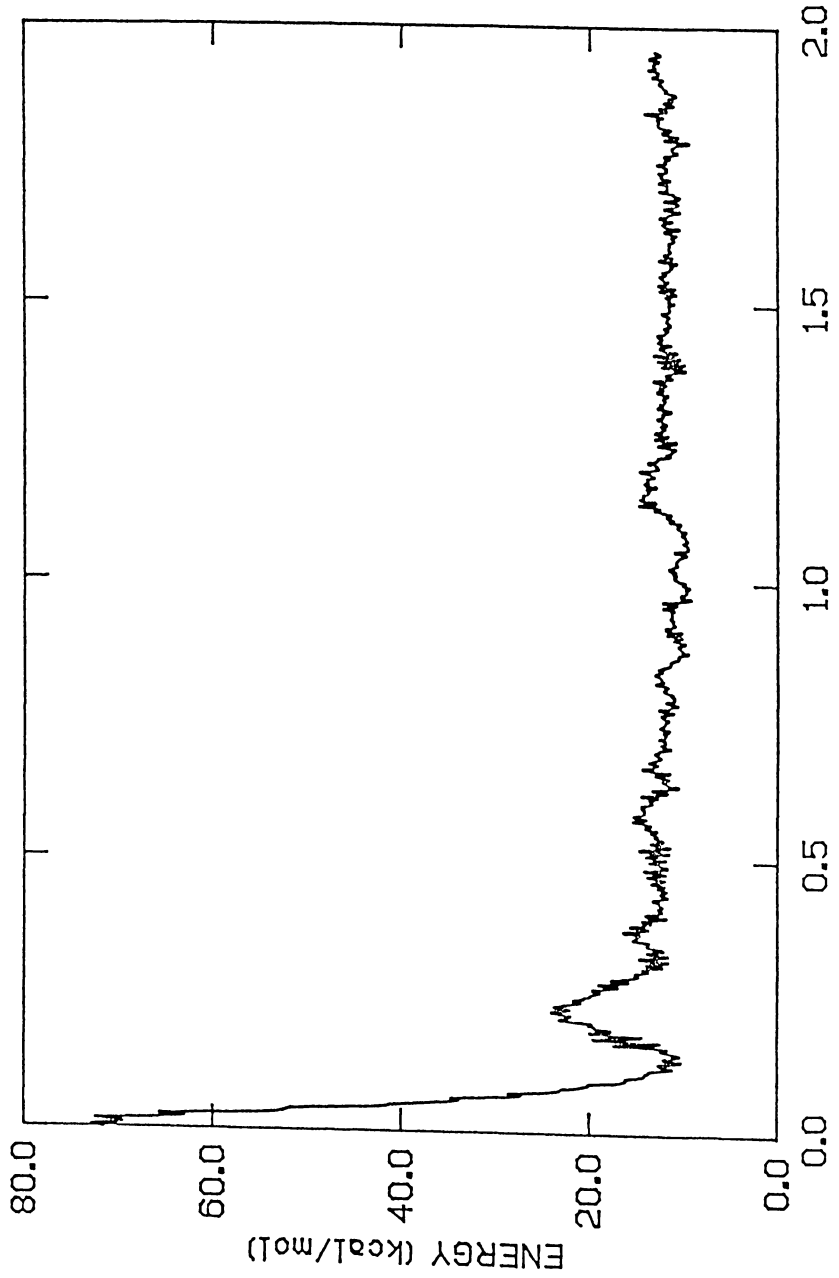

Figure 15. Same as Figure 14 except the initial CH excitation energy is 71.5 kcal/mol.

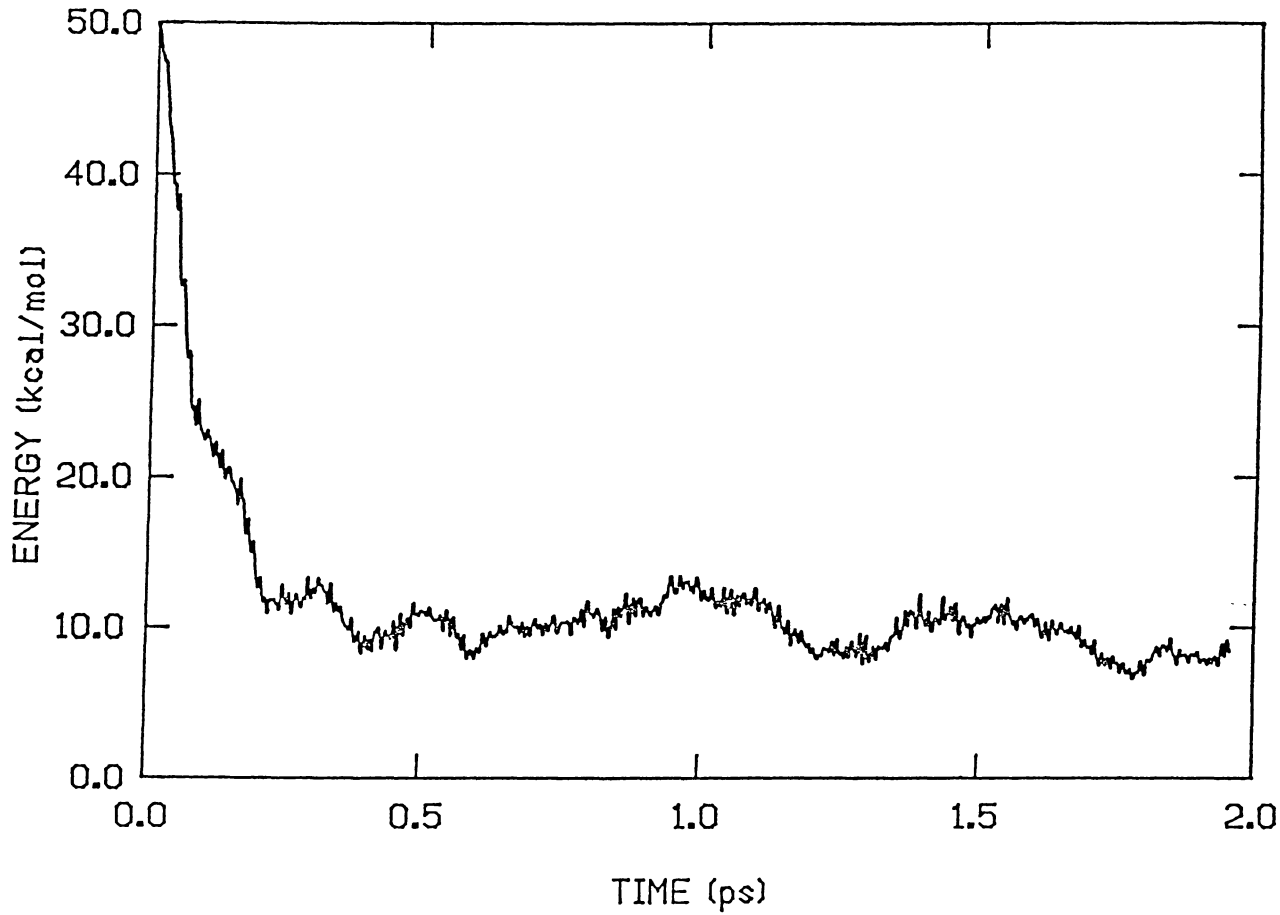

Figure 16. Same as Figure 14 except that the planar scaled force constants shown in Table VII were used.

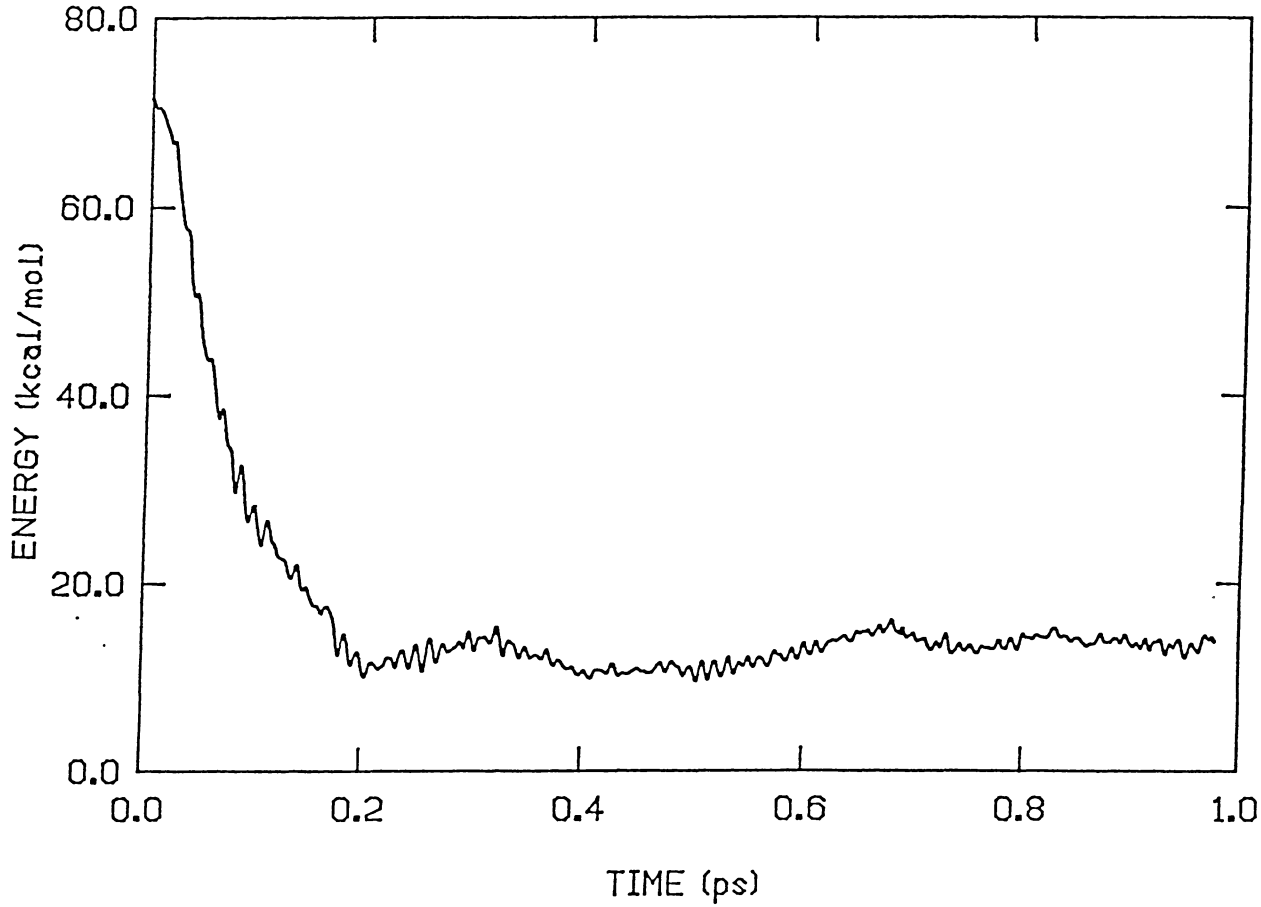

Figure 17. Same as Figure 14 except the initial excitation energy is 71.5 kcal/mol and the planar scaled force constants shown in Table VII were used.

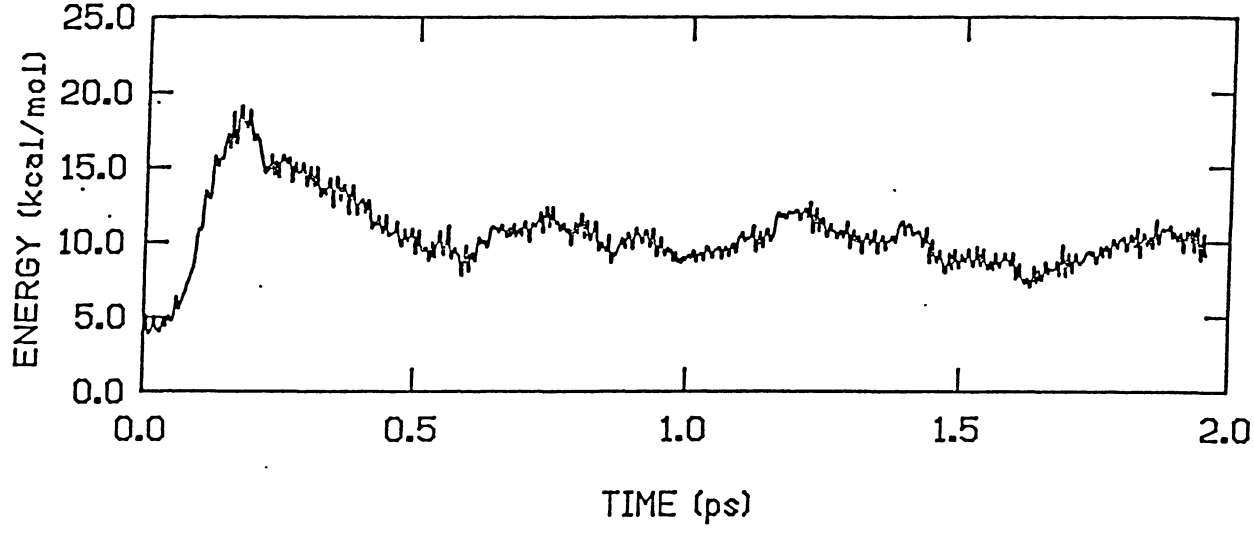

Figure 18. A plot of the average energy in the CH bond para to the initially excited CH bond as a function of time for the same ensemble in Figure 16.

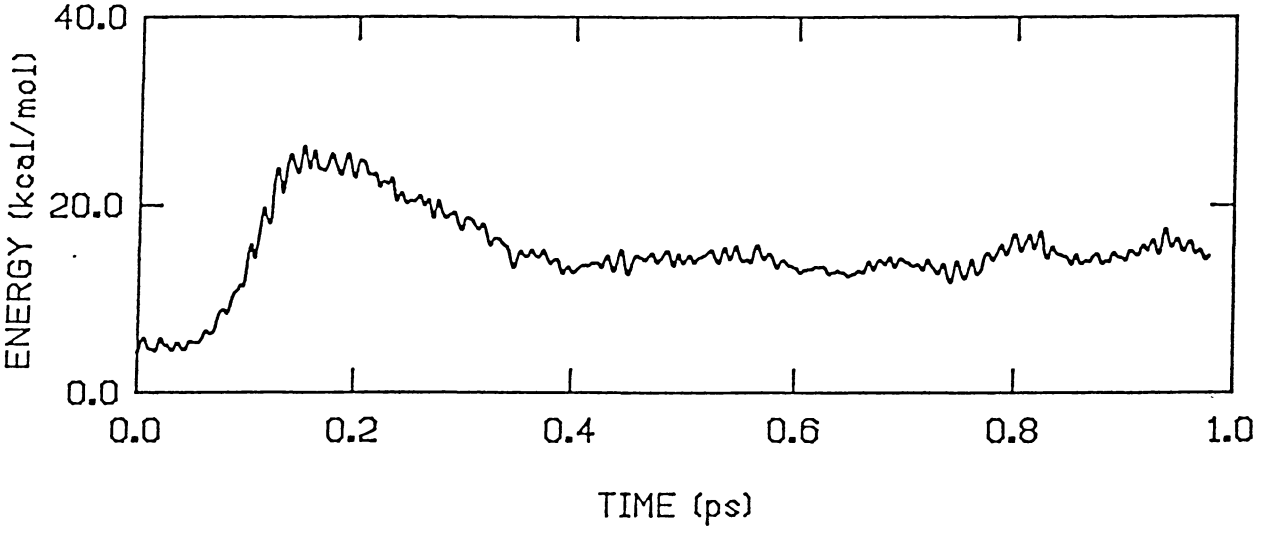

Figure 19. A plot of the average energy in the CH bond para to the initially excited CH bond as a function of time for the same ensemble as in Figure 17.

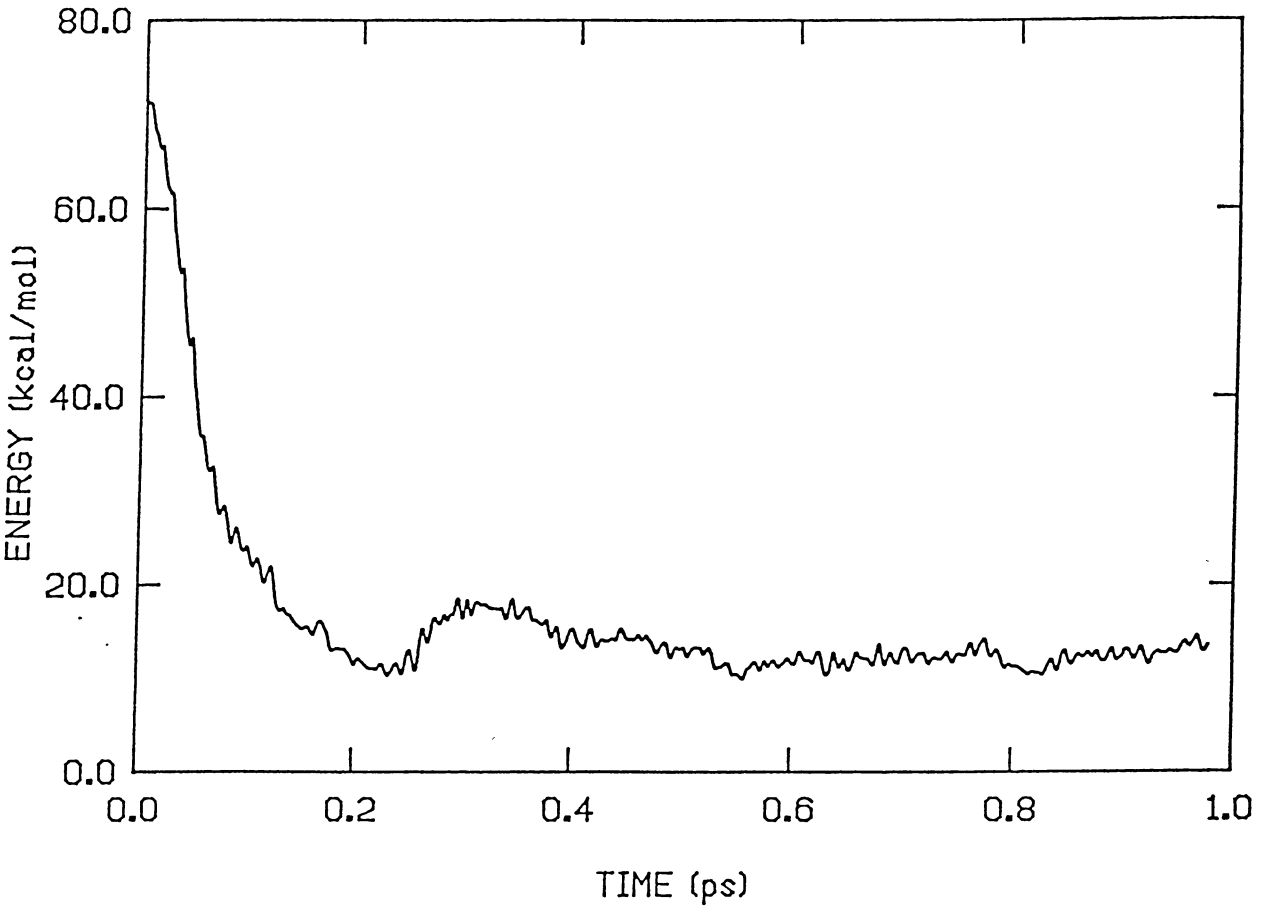

Figure 20. A plot of the average energy in the initially excited CH stretch as a function of time for an ensemble of 50 trajectories. Potential terms for out-of-plane motions were included.

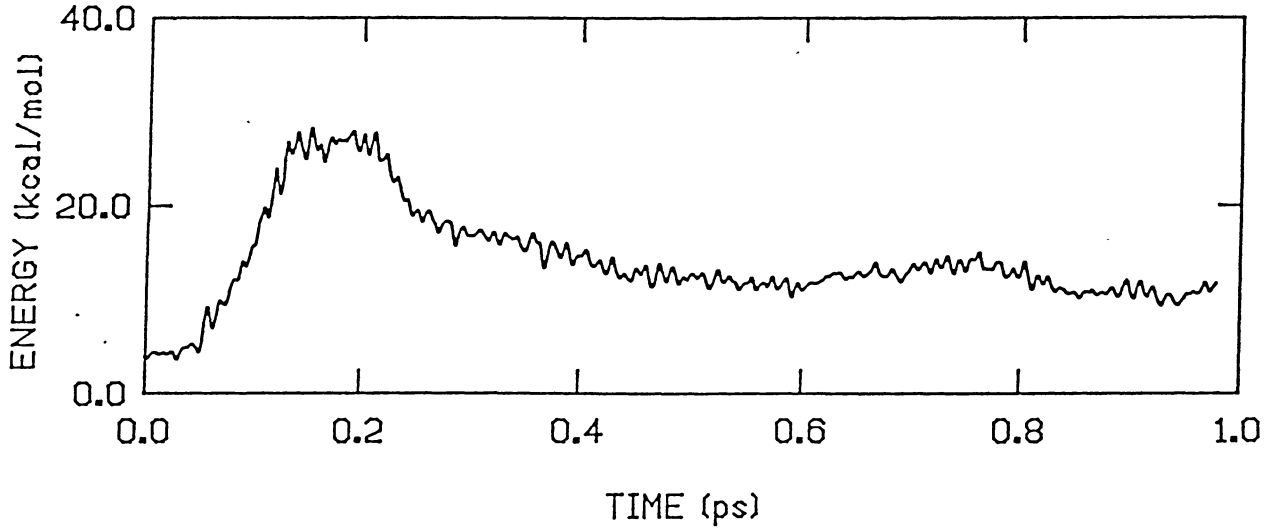

Figure 21. A plot of the average energy in the CH bond para to the initially excited CH bond as a function of time for the same ensemble as in Figure 20.

CHAPTER V

CONCLUDING REMARKS

In view of the importance of a thorough understanding of intramolecular energy transfer in highly excited large molecules, a general classical trajectory code has been developed which can be easily modified to calculate trajectories and energy transfer results for most molecules. A code of this nature allows direct simulations involving all of the motions of the molecule without major assumptions, within the limitations of the potential and the classical assumption. The results reported here are for energy transfer in benzene. The results by no means represent a complete analysis of the problem of rates and mechanisms of the energy flow. However, they do indicate that even simple potentials of the form that we have used produce results which are in qualitative agreement with experimental data, that is, energy transfer out of an initially excited local CH stretch mode is rapid and essentially irreversible. The effect of anharmonicity in increasing the rate of energy flow out of the excited bond was noted in comparing potentials 1 and 2 and in the results obtained with potentials 3-6. The results of potentials 3-6 indicate that it is necessary to treat the

coordinates which are directly involved in the energy transfer process (i.e. at or near the site of excitation) anharmonically. However, the results of potentials 7 and 8 indicate that the form of the potential can also play an important role in the energy transfer results obtained.

The objective of this work was to carry out a thorough investigation of the intramolecular energy flow in selected large molecules. It is hoped that the results of these studies will give insight into the problems of intramolecular energy redistribution and mode-specific chemistry.

BIBLIOGRAPHY

1. C. J. Cerjan, S. Shi, and W. H. Miller, J. Phys. Chem. 86, 2244(1982).

2. S. Shi and W. H. Miller, Theor. Chim. Acta 68, 1(1985).

3. D. F. Heller and S. Mukamel, J. Chem. Phys. 70, 463(1979).

4. V. Buch, R. B. Gerber, and M. A. Ratner, J. Chem. Phys. 81, 3393(1984).

5. E. L. Sibert, J. T. Hynes, and W. P. Reinhardt, J. Chem. Phys. 81, 1135(1984).

6. E. L. Sibert, W. P. Reinhardt, and J. T. Hynes, J. Chem. Phys. 81, 1115(1984).

7. E. L. Sibert, J. S. Hutchinson, J. T. Hynes, and W. P. Reinhardt, in Ultrafast Phenomena IV, edited by D. H. Auston and K. B. Eisenthal (Springer-Verlag, New York, 1984), p. 336.

8. E. L. Sibert, W. P. Reinhardt, and J. T. Hynes, Chem. Phys. Lett. 92, 455(1982).

9. P. R. Stannard and W. M. Gelbart, J. Phys. Chem 85, 3592(1981).

10. K. V. Reddy, D. F. Heller, and M. J. Berry, J. Chem. Phys. 76, 2814(1982).

11. T. A. Holme and J. S. Hutchinson, J. Chem. Phys. 84, 5455(1986).

12. F. F. Crim, Ann. Rev. Phys. Chem. 35, 657(1984).

13. M. C. Flowers and B. S. Rabinovitch, J. Phys. Chem 89, 563(1985).

14. C. S. Parmenter, Faraday Discuss. Chem. Soc. 75, 7(1983).

15. J. B. Hopkins, P. R. R. Langridge-Smith, and R. E. Smalley, J. Chem. Phys. 78, 3410(1983).

16. R. E. Smalley, J. Phys. Chem. 86, 3504(1982).

17. K. N. Swamy and W. L. Hase, J. Chem. Phys. 82, 123(1985).

18. J. D. McDonald, Ann. Rev. Phys. Chem. 30, 29(1979).

19. G. M. Stewart and J. D. McDonald, J. Chem. Phys. 75, 5949(1981); G. M. Stewart and J. D. McDonald, J. Chem. Phys. 78, 3907(1983).

20. D. W. Oxtoby and S. A. Rice, J. Chem. Phys. 65, 1676(1976).

21. V. Lopez and R. A. Marcus, Chem Phys. Lett. 93, 232(1982).

22. T. Uzer and J. T. Hynes, J. Phys. Chem. 90, 3524(1986).

23. H. Goldstein, "Classical Mechanics", Addison-Wesley, New York, (1980).

24. E. B. Wilson, Jr., J. C. Decius, and P. C. Cross, "Molecular Vibrations", Dover, New York, (1980).

25. H. H. Suzakawa, Jr., D. L. Thompson, V. B. Cheng, and M. Wolfsberg, J. Chem. Phys. 59, 4000(1973).

26. W. L. Hase, D. G. Buckowski, and K. N. Swamy, J. Phys. Chem. 87, 2754(1983).

27. E. R. Heineman, "Plane Trigonometry", McGraw-Hill, New York, (1980).

28. M. L. Boas, "Mathematical Methods in the Physical Sciences", Wiley, New York, (1983).

29. F. P. Beer and E. R. Johnston, Jr., "Vector Mechanics for Engineers", McGraw-Hill, New York, (1977).

30. D. A. McQuarrie, "Statistical Mechanics", Harper & Row, New York, (1976).

31. P. Pulay, G. Fogarasi, and J. E. Boggs, J. Chem. Phys. 74, 3999(1981).

32. P. J. Nagy and W. L. Hase, Chem. Phys. Lett. 54, 73(1978).

33. P. J. Nagy and W. L. Hase, Chem. Phys. Lett. 58, 482 (E) (1978).

34. T. Shimanouchi, Natl. Stand. Ref. Data Ser. Natl. Bur. Stand. 39, Consolidated Vol. 1, 152(1972).

35. A. G. Ozkabak, L. Goodman, S. N. Thakur, and K. Krogh-Jespersen, J. Chem. Phys. 83, 6047(1985).

36. S. Brodersen and A. Langseth, K. Dan. Vidensk. Selsk. Mat.-Fys. Sk. 1, No. 1(1956).

VITA

KAREN LYNN BINTZ

Candidate for the Degree of

Master of Science

Thesis: CLASSICAL DYNAMICS STUDY OF INTRAMOLECULAR ENERGY TRANSFER IN BENZENE

Major Field: Chemistry

Biographical:

Personal Data: Born in Pryor, Oklahoma, March 31, 1960, the daughter of Jack T. and Thelma L. Walker. Married to Daniel G. Bintz, O. D., on December 22, 1985.

Education: Graduated from Pryor High School, Pryor, Oklahoma, in May, 1978; received Bachelor of Science Degree in Chemistry from Northeastern Oklahoma State University, Tahlequah, Oklahoma, in May, 1984; completed requirements for the Master of Science degree at Oklahoma State University in December, 1986.

Professional Experience: Teaching Assistant, Department of Chemistry, Oklahoma State University, August, 1984, to May, 1984; Research Assistant, Department of Chemistry, Oklahoma State University, June, 1984, to September, 1986.